

A Dual-AoI-based Approach for Optimal Transmission Scheduling in Wireless Monitoring Systems with Random Data Arrivals

Yuchong Zhang, *Graduate Student Member, IEEE*, Yi Cao, Xianghui Cao, *Senior Member, IEEE*

Abstract—In Internet of Things (IoTs), the freshness of system status information is crucial for real-time monitoring and decision-making. This paper studies the transmission scheduling problem in wireless monitoring systems, where information freshness—typically quantified by the Age of Information (AoI)—is heavily constrained by limited channel resources and influenced by factors such as the randomness of data arrivals and unreliable wireless channel. Such randomness leads to asynchronous AoI evolution at local sensors and the monitoring center, rendering conventional scheduling policies that rely solely on the monitoring center’s AoI inefficient. To this end, we propose a dual-AoI model that captures asynchronous AoI dynamics and formulate the problem as minimizing a long-term time-average AoI function. We develop a scheduling policy based on Markov decision process (MDP) to solve the problem, and analyze the existence and monotonicity of a deterministic stationary optimal policy. Moreover, we derive a low-complexity scheduling policy which exhibits a channel-state-dependent threshold structure. In addition, we establish a necessary and sufficient condition for the stability of the AoI objective. Simulation results demonstrate that the proposed policy outperforms existing approaches.

Index Terms—Wireless monitoring, data freshness, dual-AoI, Markov decision process, random data arrivals.

I. INTRODUCTION

IN recent years, the Internet of Things (IoTs) has developed rapidly and has been widely applied in various domains, including smart manufacturing, intelligent transportation and environmental monitoring [1]–[3]. In IoT applications, the status information is fundamental, which necessitates real-time monitoring of the underlying physical processes. Utilizing outdated status may lead to incorrect decisions or even catastrophic consequences, thus it is crucial to maintain timely status awareness.

As a network performance metric for quantifying information freshness, the age of information (AoI) has been proposed and attracted increasing attention, which is defined as the time elapsed since the most recently received update packet was generated [4]. It is worth noting that the loss of information value in IoT systems typically exhibits a nonlinear trend instead of the linear characteristic of AoI. For instance, in remote control systems, the control errors

or safety risks induced by the increase of AoI may grow exponentially [5]. This motivates the use of an AoI function to map the time metric to information urgency, enabling a more accurate evolution of the penalty associated with AoI updates in the decision-making process. On the other hand, the common “generate-at-will” model assumes that the sensor always possesses fresh data ready for transmission [6], but data arrivals are sometimes random, where fresh data packets may be unavailable at the time of scheduling. Specifically, such random data arrival is prevalent in practical network sensing applications and there exist the following three typical scenarios: 1) *Random observation*, in vehicle networks, some sensors generate update packets based on specific events, i.e., vehicle motion causes changes in distance or speed [7]; 2) *Random energy availability*, in energy-harvesting environmental monitoring, data generated by sensors deployed in fields may be available in a random manner due to the random nature of energy harvesting processes [8]; 3) *Random access*, in random access networks, contention-based data transmission may result in random data arrivals [9]. Therefore, the sensor-side uncertainty induced by random data arrivals is a non-negligible issue in scheduling policy design.

The randomness in data arrivals may cause conventional deterministic scheduling methods to overlook the fact that no fresh data is available at the sensor-side during scheduling, thereby leading to inefficient decision-making [10]. As a result, scheduling decisions should consider not only the AoI at the monitoring center (MC) but also the sensor-side data arrival state. In addition, a high AoI at the MC does not necessarily mean that a new update from sensor is worthwhile, since the data packet stored in the buffer may still be stale, which forces the scheduler to make decisions between transmitting an older packet currently or foregoing the scheduling opportunity. Accordingly, both sensor-side data availability and buffered data freshness need to be jointly accounted for.

Furthermore, the randomness of wireless channels introduces a new challenge to this scheduling problem. When the channel quality is poor, a scheduled sensor may not be able to deliver its update packets successfully. Moreover, in practical network transmissions, channel quality may vary dynamically, possessing temporal correlation, and cannot be accurately characterized by the commonly adopted independent and identically distributed (i.i.d.) channel models [11]. In this case, data arrivals may occur when channel condition is poor, while good transmission windows may appear when no fresh data is available, requiring the scheduler to trade off

Y. Zhang and X. Cao are with the School of Automation, Southeast University, and Key Laboratory of Measurement and Control of Complex Systems of Engineering, Ministry of Education, Nanjing 210096, China (e-mail: yc_zhang@seu.edu.cn, xhcao@seu.edu.cn).

Y. Cao is with the China United Network Communications Co., Ltd., Guangzhou Branch, Guangzhou 510620, China (e-mail: caoyi12@chinaunicom.cn).

the transmission of old data packet against possible channel quality reduction upon new arrivals. Due to the randomness of wireless channels and data arrivals, the AoI at the local sensor (AoLI) and that at the receiver in MC (AoRI) evolve in a non-synchronized manner. Hence, it is essential to design a dual-AoI-aware scheduling strategy that jointly captures the effects of data arrival and wireless transmission on monitoring performance.

Motivated by the aforementioned challenges, this paper investigates a transmission scheduling problem for wireless monitoring networks over a shared memory-based channel. To capture information freshness subject to random data arrivals, we consider the asynchronous AoLI and AoRI in the transmission process of data packets from multiple local sensors to the MC, based on which we construct an AoI function of monitoring performance and formulate the optimization problem. We introduce a Markov decision process (MDP) to analyze the structure of the optimal scheduling policy and, leveraging this structural insight, design a low-complexity near-optimal scheduling framework. The main contributions of this work are summarized as follows:

- 1) We propose a dual-AoI evolution model, and formulate an optimization scheduling problem that minimizes the long-term time-average sum AoI functions.
- 2) We establish a MDP-based approximate structure of optimal policy through value function decomposition, and reveal that it exhibits a channel state-dependent threshold structure. Then, a structure-informed scheduling algorithm is presented.
- 3) We derive a necessary and sufficient condition related to data arrival rate to guarantee monitoring stability over a shared memory-based channel.

The remainder of this paper is organized as follows. In Section 2, related works are reviewed. Section 3 proposes the system model and builds the optimization problem. Section 4 constructs the MDP framework and designs the policy, as well as some theoretical results. The simulation analysis is given in Section 5. Section 6 makes the conclusion.

Notations: \mathbb{N} , \mathbb{R} and \mathbb{Z}^+ denote the sets of all non-negative integers, real numbers and positive integers, respectively. \mathbb{R}^n is the n -dimensional Euclidean space. $\Pr(\cdot)$ and $\mathbb{E}[\cdot]$ stand for the probability and expectation of stochastic events, respectively. The transposition, trace and spectral radius of matrix A are denoted by $(A)^T$, $\text{Tr}(A)$ and $\rho(A)$, respectively. $\text{diag}\{\cdot\}$ denotes the diagonal matrix. $\|\alpha\|$ is the 1-norm of vector α . Inequalities between two vectors are interpreted elementwise, expressed as \succeq or \preceq .

II. RELATED WORKS

The freshness of status updates delivered to the receiver is paramount for ensuring precise monitoring under the wireless network environment. Consequently, substantial research efforts have been dedicated to quantifying this freshness and optimizing transmission scheduling accordingly. In this section, we first discuss the fundamental developments in AoI minimization and its embedded information urgency, and subsequently investigate the impact of random data arrival models

and uncertain wireless channel characteristics on scheduling design.

To characterize the timeliness of system states, AoI has been proposed from the receiver's perspective as a network-layer metric [4]. In some early studies, such as [12] and [13], the time-average AoI of queue systems was analyzed to guide the packet updates. To fully exploit the role of AoI in evaluating the performance of status update systems, the design of AoI-based scheduling has been extensively studied. In [14], [15], the transmission scheduling mechanisms aimed at AoI optimization were investigated in single-source system scenarios. With hope to extended the AoI-aware scheduling research to multi-source systems, [6] proposed the near-optimal Max-Weight and Whittle's index policies. Considering the practical constrains in network environments, [16] introduced AoI minimization to design energy-efficient data collection scheduling policy. In [17] and [18], learning-based methods have also been applied to address AoI-optimizing scheduling problems under environmental uncertainty. Similar method was also applied in [19] to design the trajectories of uncrewed aerial vehicles jointly combined with AoI optimization. However, AoI alone is insufficient to capture the information urgency, especially the dynamics of underlying devices [20]. In terms of this issue, a metric of AoI reduction was proposed in [21] to address the multi-source information update problem. In [22], the information urgency was modeled as a function of distortion measure and relative value iteration algorithm was applied to schedule the sampling and transmission. Hence, [23]–[25] constructed nonlinear AoI penalties to guide the real-time motoring optimization. Similarly, a lightweight multi-sensor scheduler was proposed in [26] based on AoI function-based estimation system model. Unlike the linear evolution of AoI, the dynamics of AoI-based functions are more complex, making traditional AoI optimization methods difficult to adopt directly.

It is worth noting that the data generation model has a significant impact on scheduling design. The aforementioned studies mainly adopt the "generate-at-will" model, in which a fresh status update is generated immediately whenever a transmission to the receiver is assigned. As a result, scheduling decisions only need to consider the instantaneous AoI value. This assumption becomes invalid when update packets arrive randomly, making many existing methods inapplicable, thus several recent studies have begun to address this challenge. [27] developed two scheduling methods for random information arrivals with no buffer based respectively on MDP framework and Whittle's index. [28] further incorporated bandwidth constraints for this problem. In [10], queueing disciplines were considered to evaluate the impact of random arrivals on AoI. Moreover, [29] modeled the partial information uncertainty caused by random arrivals as a partially observation problem. While these works effectively address source-side uncertainty, they overlook the physical layer characteristics of wireless links, typically assuming i.i.d. channels [21]. In environments involving networks made up of multi-devices, wireless channels often exhibit temporal correlation or memory [11]. In [30], the Gilbert-Elliott (GE) model was used to describe the packet loss occurring in transmissions. As reported in

Table I. Summary and Comparison of Related Works

References	Optimization Objective	Main Methods	Items of Interest		
			Data Arrival Randomness	Channel Dynamics	Policy Stability
[14]	Time-average AoI	MDP, relative value iteration	X	X	X
[15]	Time-average AoI and energy	MDP, Q-learning	X	X	X
[18]	Weighted sum average AoI	Constrained MDP, threshold-based policy	X	X	X
[19]	Peak AoI	MDP, deep reinforcement learning	X	X	X
[21]	Time-average AoI penalty	Greedy algorithm	X	X	X
[22]	Time-average AoI penalty	MDP, deep reinforcement learning	✓	X	X
[24]	Average AoI penalty	Theoretical method	X	X	X
[25]	Time-average AoI penalty and energy	MDP, theoretical method	X	X	✓
[26]	Time-average AoI function	MDP, Whittle-index	X	X	✓
[27]	Time-average AoI	MDP, relative value iteration	✓	X	X
[28]	Time-average AoI	MDP, relative value iteration	✓	✓	X
[29]	Time-average AoI	MDP, Max-Weight policy	✓	X	X
[30]	Time-average error and energy	MDP, relative value iteration	X	✓	✓
[31]	Time-average error and energy	MDP, relative value iteration	X	✓	✓
[32]	Time-average AoI-realated value	MDP, deep reinforcement learning	X	X	X
[33]	AoI penalty	Constrained MDP, relative value iteration	✓	X	X
[34]	Time-average AoI	Constrained MDP, Lyapunov optimization	✓	X	X
This Work	Time-average dual-AoI function	MDP, structure analysis, low-complexity theoretical method	✓	✓	✓

[31], this memory was modeled as a Markov chain and studied the transmission stability problem for single system scenarios. Thus, it remains an open problem that how to account for the effects of random data arrivals and ensure both the timeliness and stability of monitoring coupled with memory-based channels.

The summary of related works are listed in Table I. In contrast to our work, most existing studies focus primarily on minimizing the AoI value itself, without exploiting the information urgency expression of AoI-based performance functions. Although MDP formulations are widely used, the structural design of scheduling policies remains underexplored. Furthermore, by jointly accounting for stochastic arrivals and dynamic channels, our framework introduces new challenges for policy stability analysis.

III. SYSTEM MODEL AND PROBLEM FORMULATION

As shown in Fig. 1, we consider a typical wireless monitoring networks, where the RMC carries the real-time monitoring through acquiring data transmitted from N local sensors. Each sensor performs the local observation of an independent physical system, generates observation packets randomly, and transmits them to the RMC over a shared wireless channel. Considering the randomness of data transmission, a buffer is configured to store the freshest data packet, which means that the older data packet would be replaced upon the arrival of a newer packet. Set $i \in \mathcal{N} = \{1, 2, \dots, N\}$ as the index of local sensor, and the index of time slot is defined as $k \in \{1, 2, \dots, T\}$.

A. Memory-based Channel Model

In the wireless network environment, obstructions, reflections, or network conditions may cause dynamic variations or fading of transmission channel quality. The static channel models, i.e., independent Bernoulli distribution, commonly used in existing studies, fail to explain such phenomenon. In this case, the change of channel quality is not completely random but exhibits temporal correlations. To capture this channel memory characteristic, we introduce the GE model,

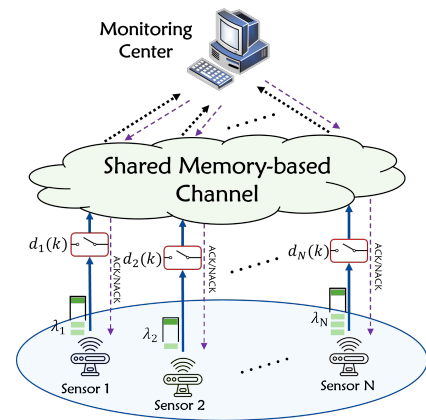


Fig. 1. The structure of wireless monitoring.

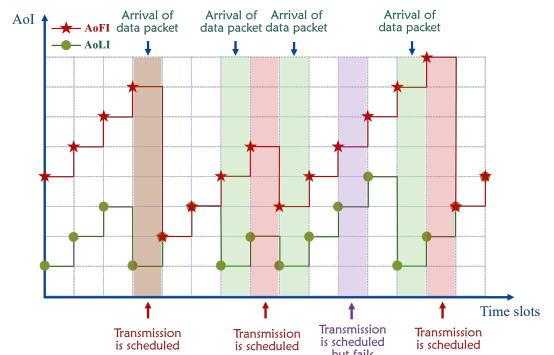


Fig. 2. Illustration of AoLI and AoFI.

which is widely applied to describe the packet loss in practical wireless networks and confirmed to represent Rayleigh-fading channels accurately [30], [35]. The channel fluctuates between "Good" and "Bad" states, naturally viewed as a two-state Markov chain, where two states are denoted by $\vartheta(k) = 1$ and $\vartheta(k) = 0$ at time slot k . The transition probabilities of

channel states are defined as follows:

$$\begin{aligned} \Pr\{\vartheta(k) = 0 | \vartheta(k-1) = 0\} &= \kappa_{00}, \\ \Pr\{\vartheta(k) = 1 | \vartheta(k-1) = 0\} &= \kappa_{01}, \\ \Pr\{\vartheta(k) = 1 | \vartheta(k-1) = 1\} &= \kappa_{11}, \\ \Pr\{\vartheta(k) = 0 | \vartheta(k-1) = 1\} &= \kappa_{10}, \end{aligned} \quad (1)$$

where $\kappa_{00}, \kappa_{01}, \kappa_{11}, \kappa_{10} \in (0, 1)$ are given transition probabilities. Besides, the probabilities of switching different states are computed by $\kappa_{01} = 1 - \kappa_{00}$ and $\kappa_{10} = 1 - \kappa_{11}$. Define $\theta_i(k)$ as an indicator of data reception at time slot k when sensor i is chosen to transmit data, i.e., $\theta_i(k) = 1$ means that data is received by MC, otherwise, $\theta_i(k) = 0$. Then, the successful transmission probability of sensor i is denoted as

$$p_i^\vartheta(k) = \Pr\{\theta_i(k) = 1 | \vartheta(k), d_i(k) = 1\}, \quad (2)$$

where $d_i(k)$ represents the scheduling decision for sensor i . Specifically, when sensor i is scheduled, $d_i(k) = 1$; otherwise, $d_i(k) = 0$. The packet loss probability of the i -th sensor is expressed as $1 - p_i^\vartheta(k)$. Moreover, we assume that the ACK/NACK signals are feedback to sensors from the MC with neglecting the delay to inform whether the transmission is successful or not.

Since the bandwidth limitation of the shared channel, it is impossible to transmit data from all sensors in each time slot. Therefore, the following constraint is proposed for the scheduling problem:

$$\sum_{i=1}^N d_i(k) \leq M, \forall k \in \mathbb{N}, \quad (3)$$

which means that at most M out of N sensors can be selected.

B. AoI Function Regarding Monitoring Performance

The existing researches mainly focus on the case where updated data packets are directly sent to destination upon generation, which is only appropriate for the sensors with stable transmission. In this paper, we consider a more general scenario of wireless monitoring networks that data packets are randomly available for transmissions. Considering the asynchronous variation in information freshness caused by the random update of data packets, it is hard to conduct the scheduling decisions based solely on the directly observed AoI, because the potential benefit of scheduling cannot be inferred. Hence, we divide the AoI evolution into two stages for analysis: AoLI and AoRI. Here we use a buffer to store the most recently available data packet. As reported in [10], the queue mechanism with only single packet can achieve the best freshness under random arrivals.

Let $\Delta_i^L(k)$ denotes the state of AoLI, measuring the elapsed time after the last update packet of local data arriving at the buffer, and $\gamma_i^L(k)$ as an indicator to show whether updated data packet arrives at buffer for sensor i . If there is no update arrival, $\gamma_i^L(k) = 0$, $\Delta_i^L(k)$ will increase by one at the beginning of next time slot, otherwise the old packet is replaced by a fresh one and $\Delta_i^L(k)$ is reset to zero with $\gamma_i^L(k) = 1$. The network-induced events follow a stochastic process, such that the arrival rate is supposed as i.i.d. for each

time slot and various sensors, which is modeled as a Bernoulli distribution with probability λ_i , i.e., $\Pr\{\gamma_i^L = 1\} = \lambda_i, i \in \mathcal{N}$. The AoLI is modeled as follows:

$$\Delta_i^L(k) = \begin{cases} 0, & \text{if } \gamma_i^L(k) = 1, \\ \Delta_i^L(k-1) + 1, & \text{if } \gamma_i^L(k) = 0. \end{cases} \quad (4)$$

When local data from sensor i is chosen to transmit and succeed, the current data packet of the i -th buffer reaches the MC, so that AoRI is updated to $\Delta_i^R(k-1) + 1$. If not, AoRI would increase by one. In view of scheduling decisions and channel qualities, we introduce an indicator $\gamma_i^R(k)$ to represent the real-time situation of data reception for sensor i , denoted as

$$\gamma_i^R(k) = d_i(k)\theta_i(k). \quad (5)$$

Then, the AoRI dynamics is described as follows:

$$\Delta_i^R(k) = \begin{cases} \Delta_i^R(k-1) + 1, & \text{if } \gamma_i^R(k) = 1, \\ \Delta_i^R(k-1) + 1, & \text{if } \gamma_i^R(k) = 0. \end{cases} \quad (6)$$

where $\Delta_i^R(k)$ measures the time elapsed since the update packet was generated. The evolution processes of AoLI and AoRI are plotted in Fig. 2.

In order to reveal the influence of information freshness on monitoring performance, we introduce the AoI function $f(\cdot)$ to measure the information urgency. Depending on system characteristics, various AoI functions have been established in the existing literature. [24] proposed a monotone non-decreasing function in the exponential form to depict the performance of universal nonlinear system. In addition, similar function was developed in [25] for remote control. Then, two typical examples are given as below:

Example 1. In many real-time network applications, such as multi-user status monitoring in V2X interconnection, online learning relies heavily on fresh data [23]. To reflect the data urgency, a commonly used AoI-penalty function is defined as

$$f(\Delta_i^R(k)) = e^{r\Delta_i^R(k)} - 1, \quad (7)$$

where $r > 0$ is a given constant.

Example 2. In typical remote state estimation systems, sensor networks can perform the local estimation using Kalman filtering. Consider a discrete-time linear time-invariant model as the monitoring object, then the estimation performance is mapped to the following function [26]:

$$f(\Delta_i^R(k)) = \text{Tr}(h^{\Delta_i^R(k)}(\bar{P}_i)), \quad (8)$$

where the function $h(\bar{P}_i) \triangleq A_i \bar{P}_i A_i^T + \Sigma_i^\omega$, $h^n(\cdot) = h(h^{n-1}(\cdot))$ and \bar{P}_i is a steady-state after long run. A_i represents the system matrix and Σ_i^ω is the covariance matrix of system process noise. Specially, (8) is easy to be expanded as $\text{Tr}\left(A_i^{\Delta_i^R(k)} \bar{P}_i (A_i^T)^{\Delta_i^R(k)} + \sum_{l=0}^{\Delta_i^R(k)-1} A_i^l \Sigma_i^\omega (A_i^T)^l\right)$.

C. Problem Formulation

In order to find a scheduling policy that can improve monitoring performance defined by AoI function, we define the cost function of the i -th sensor as $f(\Delta_i^R(k))$. The mapping

relationship from the state to the action is defined as $\pi \in \Pi$. Then, the optimization problem over infinite time horizon is formulated as follows:

Problem 1.

$$\min_{\pi \in \Pi} \limsup_{T \rightarrow \infty} \frac{1}{T} \sum_{k=1}^T \sum_{i=1}^N \mathbb{E}[f(\Delta_i^R(k))], \quad (9)$$

$$s.t. \quad (3) \text{ holds.} \quad (10)$$

IV. THE PROPOSED SCHEDULING POLICY

In this section, we first formulate the MDP based on the optimization Problem 1 in Section III. Then, we investigate the existence and structure of the optimal scheduling policy and, on this basis, develop a structure-informed scheduling policy with low complexity. Finally, the condition for ensuring the stability of monitoring performance is analyzed.

A. MDP Formulation

We assume that state evolution of AoLI and AoRI are both observable to the MC before each scheduling decision. According to Problem 1, we consider the system state consisting of AoLI $\Delta_i^L(k)$, AoRI $\Delta_i^R(k)$ and channel state $\vartheta(k)$, which varies only relying on the current state and decision instead of historical states. Therefore, the scheduling problem can be regarded as a MDP characterized by a quadruple $(\mathcal{S}, \mathcal{A}, \Pr\{\cdot|\cdot, \cdot\}, c(\cdot, \cdot))$ and details are as follows:

- The state space \mathcal{S} includes all possible values of AoLI $\Delta_i^L(k)$, AoRI $\Delta_i^R(k)$ for all sensors and channel state $\vartheta(k)$, denoted as $s(k) = (s^\Delta(k), \vartheta(k))$, where $s^\Delta(k) = (s_1^\Delta(k), s_2^\Delta(k), \dots, s_N^\Delta(k))$ and $s_i^\Delta(k) = (\Delta_i^L(k), \Delta_i^R(k)), i \in \mathcal{N}$.
- The action space \mathcal{A} consists of all feasible scheduling decisions, which is expressed as $d(k) = (d_1(k), d_2(k), \dots, d_N(k)) \in \{0, 1\}^N, d(k) \in \mathcal{A}$.
- The transition function is related to the probabilities of random arrivals and successful transmissions. According to the action taken in the current time slot, the state transits to a new state in the next time slot with the following transition probability:

$$\begin{aligned} & \Pr\{s(k) | s(k-1), d(k)\} \\ &= \Pr\{\vartheta(k) | \vartheta(k-1)\} \\ & \quad \times \Pr\{s^\Delta(k) | s^\Delta(k-1), \vartheta(k-1), d(k)\} \\ &= \Pr\{\vartheta(k) | \vartheta(k-1)\} \\ & \quad \times \prod_{i=1}^N \Pr\{s_i^\Delta(k) | s_i^\Delta(k-1), \vartheta(k-1), d_i(k)\}, \quad (11) \end{aligned}$$

where the first term only follows the Markov chain defined in (1), and it is denoted as

$$\begin{aligned} & \Pr\{\vartheta(k) | \vartheta(k-1)\} \\ &= \begin{cases} \kappa_{00}, & \text{if } \vartheta(k) = 0, \vartheta(k-1) = 0, \\ 1 - \kappa_{00}, & \text{if } \vartheta(k) = 0, \vartheta(k-1) = 1, \\ \kappa_{11}, & \text{if } \vartheta(k) = 1, \vartheta(k-1) = 1, \\ 1 - \kappa_{11}, & \text{if } \vartheta(k) = 1, \vartheta(k-1) = 0, \\ 0, & \text{otherwise.} \end{cases} \quad (12) \end{aligned}$$

Then, the second term in the right-hand side (RHS) of (11) is given by

$$\begin{aligned} & \Pr\{s_i^\Delta(k) | s_i^\Delta(k-1), \vartheta(k-1), d_i(k)\} \\ &= \begin{cases} \lambda_i p_i^\vartheta(k), & \text{if case (1),} \\ (1 - \lambda_i) p_i^\vartheta(k), & \text{if case (2),} \\ \lambda_i (1 - p_i^\vartheta(k)), & \text{if case (3),} \\ (1 - \lambda_i) (1 - p_i^\vartheta(k)), & \text{if case (4),} \\ \lambda_i, & \text{if case (5),} \\ 1 - \lambda_i, & \text{if case (6),} \\ 0, & \text{otherwise,} \end{cases} \quad (13) \end{aligned}$$

where $p_i^\vartheta(k)$ represents the successful transmission probability under channel state $\vartheta(k-1)$ for sensor i . The above six possible cases are listed as follows:

- case (1): $d_i(k) = 1, s_i^\Delta(k) = (0, \Delta_i^L(k-1) + 1)$,
- case (2): $d_i(k) = 1, s_i^\Delta(k) = (\Delta_i^L(k-1) + 1, \Delta_i^L(k-1) + 1)$,
- case (3): $d_i(k) = 1, s_i^\Delta(k) = (0, \Delta_i^R(k-1) + 1)$,
- case (4): $d_i(k) = 1, s_i^\Delta(k) = (\Delta_i^L(k-1) + 1, \Delta_i^R(k-1) + 1)$,
- case (5): $d_i(k) = 0, s_i^\Delta(k) = (0, \Delta_i^R(k-1) + 1)$,
- case (6): $d_i(k) = 0, s_i^\Delta(k) = (\Delta_i^L(k-1) + 1, \Delta_i^R(k-1) + 1)$.

- The one-step cost function is obtained from the given action and state. Thus, according to Problem 1, the one-step cost of MDP is defined as $c(s(k), d(k)) = \sum_{i=1}^N f(\Delta_i^R(k))$.

Given a scheduling policy π , the time-average cost function with an initial state s_0 is written as

$$\mathcal{C}(s_0, \pi) = \limsup_{T \rightarrow \infty} \frac{1}{T} \sum_{k=1}^T \mathbb{E}[c(s(k), d(k)) | s_0, \pi]. \quad (14)$$

Hence, the optimization problem is equivalent to find a policy minimizing the cost function (14), that is

Problem 2.

$$\min_{\pi \in \Pi} \mathcal{C}(s_0, \pi), \quad s.t. \quad (3) \text{ holds.} \quad (15)$$

B. Existence and Property of Deterministic Stationary Optimal Policy

According to the theory present in [36], the solution of Problem 2 corresponds to the optimal policy π^* available within the set of deterministic stationary policies, provided that the time-average cost (14) is bounded. Assume that ϕ^* is the optimal value of $\mathcal{C}(s_0, \pi)$ under any initial value $s_0 \in \mathcal{S}$, then the Bellman equation can be formulated as follows:

$$\phi^* + Q(s) = \min_{d \in \mathcal{A}} \left[c(s, d) + \sum_{s' \in \mathcal{S}} \Pr\{s' | s, d\} Q(s') \right], \quad (16)$$

where $Q(s)$ denotes the action-value function that reflects the expected objective value under the optimal policy π^* , and $\Pr\{s' | s, d\}$ is defined in (11). To simplify the expression, s'

denotes the state of next step, s and d denote $s(k)$ and $d(k)$, respectively. The optimal policy π^* is deservedly written as

$$\pi^*(s) = \arg \min_{d \in \mathcal{A}} \left[c(s, d) + \sum_{s' \in \mathcal{S}} \Pr\{s'|s, d\} Q(s') \right]. \quad (17)$$

In turn, we derive the existence theorem of deterministic stationary optimal policy based on the formulated MDP framework.

Theorem 1. *If Problem 2 is feasible, i.e., time-average cost (14) is bounded, there exist a constant ϕ^* and a function $Q(\cdot)$ such that the deterministic stationary optimal policy π^* can be obtained by solving Bellman equation (16).*

Proof. See Appendix A. \square

Remark 1. *By reducing the 0-1 knapsack problem, Problem 2 can be proven to be NP-hard. When the infinite-horizon cost $\mathcal{C}(s_0, \pi)$ is focused on finite-horizon, there exists a number \bar{C} that $\mathcal{C}(s_0, \pi) \leq \bar{C}$. The scheduling time for each sensor can be used as a weight. Minimizing the sum of AoI function via scheduling sensors is viewed as selecting knapsacks to maximize object value subject to the total time. Thus, Problem 2 is verified as a NP-hard problem. Then, MDP framework is built for this problem and Theorem 1 establishes the existence of a deterministic stationary optimal policy, whose structure is inherently determined by the action-value function $Q(s)$. Nevertheless, deriving this optimal policy requires solving the recursive relation in (16), making a closed-form characterization intractable. This motivates the need to investigate the structural property to guide the design of scheduling policy.*

Then, based on the established Bellman equation (16), the monotonicity analysis of the optimal policy π^* will be analyzed. In order to express the iteration process, the action-based cost function of the n -th iteration is defined as

$$\Theta_n(s, d) = c(s, d) + \sum_{s' \in \mathcal{S}} \Pr\{s'|s, d\} Q_n(s'). \quad (18)$$

Define $\tilde{\Delta}^L = (\Delta_i^L)_{i \in \mathcal{N}}$ and $\tilde{\Delta}^R = (\Delta_i^R)_{i \in \mathcal{N}}$. Then, we can further obtain the following lemma:

Lemma 1. *Given a channel state ϑ , for two states $s^a = (\tilde{\Delta}^{L,a}, \tilde{\Delta}^{R,a}, \vartheta)$ and $s^b = (\tilde{\Delta}^{L,b}, \tilde{\Delta}^{R,b}, \vartheta)$, there exists $Q(s^b) \geq Q(s^a)$ if $\tilde{\Delta}^{L,b} \succeq \tilde{\Delta}^{L,a}$ and $\tilde{\Delta}^{R,b} \succeq \tilde{\Delta}^{R,a}$.*

Proof. See Appendix B. \square

Lemma 1 reveals that the action-value function $Q(s)$ increases monotonically with the staleness of information under a fixed channel state. The monotonicity of $Q(s)$ theoretically explains that the optimal policy tends to schedule sensors with more outdated data. Some existing literature introduces a threshold structure to design the optimization algorithm, such as [31]. However, seeking a scheduling policy for multiple sensors possesses a high computational complexity, which motivates us to restrict the search space accordingly.

C. Structure-Informed Scheduling Policy

Inspired by the approximate dynamic programming [37], we formulate a distributed framework to decompose the optimization problem based on the structural property in Lemma 1 and decrease the complexity via introducing the randomized policy that easy to implement. We first define a scheduling policy π_R that sensors are chosen randomly with probability $p_i^R \in (0, 1)$, $i \in \mathcal{N}$, where p_i^R is constrained by $\sum_{i=1}^N p_i^R \leq M$. Then, we can further derive a linear approximated structure of the optimal policy.

Theorem 2. *There exists an approximation of the optimal policy defined in (17), denoted as follows:*

$$\tilde{\pi}^*(s) = \arg \min_{d \in \mathcal{A}} \left[c(s, d) + \sum_{s' \in \mathcal{S}} \Pr\{s'|s, d\} \sum_{i \in \mathcal{N}} Q_i^R(s'_i) \right] \quad (19)$$

where $Q_i^R(s_i)$ is the value function corresponding to sensor i under the randomized scheduling action.

Proof. See Appendix C. \square

Remark 2. *Through the linear decomposability of action-value function $Q(s)$, Theorem 2 approximates the original optimal policy while ensuring better performance than any randomized scheduling policies. Besides, similar to algorithm in [38], this approximation can effectively simplify the computation. Given $\bar{\Delta}_i^L$ and $\bar{\Delta}_i^R$ as the upper limits of AoLI and AoRI, respectively. It is evident that when $Q(s)$ is transformed into $\sum_{i \in \mathcal{N}} Q_i^R(s)$, the computation complexity is reduced to $O(\sum_{i \in \mathcal{N}} 2^{\bar{\Delta}_i^R (\bar{\Delta}_i^L + 1)})$ from $O(\prod_{i \in \mathcal{N}} 2^{\bar{\Delta}_i^R (\bar{\Delta}_i^L + 1)})$, which is linearly related to the number of sensors rather than exponentially related.*

Some works have given the threshold structure for the optimal policy hoping to reduce the computational cost [39]. Next, we further analyze the similar structural property of the approximated policy proposed in Theorem 2.

Theorem 3. *The proposed approximated optimal policy possesses a threshold structure with respect to (w.r.t.) Δ_i^R , such that there exists the following result for the i -th sensor, $i \in \mathcal{N}$:*

$$\tilde{\pi}_i^* = \begin{cases} 1, & \text{if } \Delta_i^R \geq \Delta_{0,i}^{R,*}, \vartheta = 0, \\ 1, & \text{if } \Delta_i^R \geq \Delta_{1,i}^{R,*}, \vartheta = 1, \\ 0, & \text{otherwise,} \end{cases} \quad (20)$$

where $\Delta_{0,i}^{R,*}$ and $\Delta_{1,i}^{R,*}$ are denoted as

$$\begin{aligned} \Delta_{0,i}^{R,*} &\triangleq \min\{\Delta_i^R \mid \Theta^\dagger(s, d) \leq \Theta^\dagger(s, d'), \vartheta = 0, d \neq d', d_i = 1\}, \\ \Delta_{1,i}^{R,*} &\triangleq \min\{\Delta_i^R \mid \Theta^\dagger(s, d) \leq \Theta^\dagger(s, d'), \vartheta = 1, d \neq d', d_i = 1\}, \\ \Theta^\dagger(s, d) &\triangleq c(s, d) + \sum_{s' \in \mathcal{S}} \Pr\{s'|s, d\} \sum_{i \in \mathcal{N}} Q_i^R(s'_i). \end{aligned}$$

Proof. See Appendix D. \square

Theorem 3 indicates that a sensor is to be scheduled for transmission once AoRI exceeds a threshold $\Delta_i^{R,*}$, which reflects the urgency to refresh the outdated information. Moreover, this action demonstrates a certain persistence that if $\tilde{\pi}^*(s) = 1$ under current Δ_i^R , than for any $(\Delta_i^R)' > \Delta_i^R$ there exists $\tilde{\pi}^*(s') = 1$. This provides an intuitive scheduling

Algorithm 1 Structure-Informed Scheduling Policy

Input: $N, M, \lambda_i, \bar{\Delta}_i^L, \bar{\Delta}_i^R, \varrho, p_i^R, p_i^\vartheta, \kappa_{00}, \kappa_{11}$ and n_{max} .

Output: Scheduling policy $\tilde{\pi}^*$.

```

1: for  $i = 1$  to  $N$  do
2:   Initialize  $Q_{i,n}^R(s_i) \leftarrow 0, \forall s_i \in \mathcal{S}_i, n \leftarrow 1$ ;
3:   repeat
4:     for all  $s_i \in \mathcal{S}_i$  do
5:        $Q_{i,n+1}^R(s_i) \leftarrow f(\Delta_i^R)$ 
6:        $+ \sum_{s'_i \in \mathcal{S}_i} \mathbb{E}^{\pi^R}[\text{Pr}\{s'_i | s_i, d_i\}] Q_{i,n+1}^R(s'_i)$ ;
7:        $Q_{i,n+1}^R(s_i) \leftarrow Q_{i,n+1}^R(s_i) - Q_{i,n+1}^R(s_i^r)$ ;
8:     end for
9:      $n \leftarrow n + 1$ ;
10:    until  $\|Q_{i,n}^R(s_i) - Q_{i,n-1}^R(s_i^r)\| \leq \varrho$  or  $n = n_{max}$ ;
11:  end for
12:  for all  $s \in \mathcal{S}$  do
13:    if  $\exists i \in \mathcal{N}$  and  $s' \in \mathcal{S}$  such that  $\tilde{\pi}^*(s') = d \in \mathcal{A}$  with
14:     $d_i = 1, \bar{\Delta}^L = \bar{\Delta}^{L'}, \vartheta = \vartheta'$  and  $\Delta_i^R \geq \Delta_i^{R'}$  only for
15:    the  $i$ -th sensor, then
16:       $\tilde{\pi}^*(s') \leftarrow d$ ;
17:    else
18:      Obtain  $\tilde{\pi}^*(s')$  by (19);
19:    end if
20:  end for
21: return Scheduling policy  $\tilde{\pi}^*$ .
    
```

rule that allows efficient implementations without solving the full MDP. The proposed structure-informed scheduling policy (SISP) is shown in Algorithm 1, which operates in two main phases. In lines 1-10, the relative value iteration algorithm is employed to update the i -th decomposed value function $Q_i^R(s_i)$ proposed in Theorem 2, where $Q_{i,n}^R(s_i)$ is the n -th iteration and a reference state s_i^r is used for normalization in line 6 to ensure numerical stability. Lines 11-17 constructs the optimal policy $\tilde{\pi}^*$, where the threshold structure proved in Theorem 3 is utilized. It is obvious that the scheduling decision is made directly if the condition in line 12 is meet and this structure-informed pruning significantly reduces the computational overhead.

D. Stability Analysis of the Monitoring Performance

In this section, we analyze the conditions required to ensure the convergence of monitoring performance. Due to the uncertainties introduced by random data arrivals and fluctuating channel states, it is difficult to maintain consistently successful update transmissions, which may worsen the monitoring performance. Therefore, it is necessary to identify the range of transmission probabilities and random arrival rates that can guarantee stable monitoring, thereby providing a guidance for the design of real remote monitoring networks.

For the scenario of a single sensor system, studies in [30] and [31] have analyzed the conditions for ensuring the stability of remote state estimation under Markov channel states, but this class of theoretical results cannot be directly applied to the network system consisting of multiple sensors. In [26], the stability conditions of remote state estimation in multi-sensor

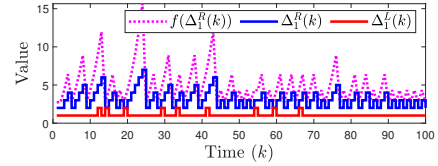
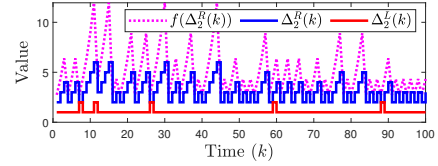
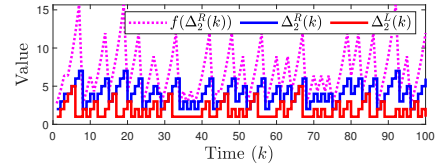

 (a) Sensor 1 with $\lambda_1 = 0.9$.

 (b) Sensor 2 with $\lambda_2 = 0.9$.

 (c) Sensor 2 with $\lambda_2 = 0.5$.

Fig. 3. The evolution of AoI function, AoLI and AoRI for two sensors.

systems have been investigated, while channel is limited to be static and the impact of random data arrivals is neglected. Referring to the threshold structure proposed in Theorem 3, we utilize the limitation distribution of the value of Δ_i^R to derive the sufficient and necessary condition for the stable monitoring performance. To pursue a more universal result, we consider the more complex AoI function introduced in Example 2.

Theorem 4. For the AoI function defined in (8), the time-average cost $\mathcal{C}(s_0, \pi)$ is bounded under the proposed scheduling policy $\tilde{\pi}^*$ if and only if the following condition is satisfied:

$$\rho(\Omega(I - \lambda_i \mathcal{P}_i)) < \frac{1}{\rho^2(A_i)}, \forall i \in \mathcal{N}, \quad (21)$$

where $\Omega = \begin{bmatrix} \kappa_{00} & \kappa_{01} \\ \kappa_{10} & \kappa_{11} \end{bmatrix}$ and $\mathcal{P}_i = \text{diag}\{p_i^0, p_i^1\}$.

Proof. See Appendix E. \square

Remark 3. According to the form of (21), we observe that monitoring performance can only be maintained if transmission channels are sufficiently reliable to match the rate at which data arrive, providing the guidance for the design of wireless monitoring networks. Using the same method, a corollary is further derived for the AoI function defined in Example 1. Moreover, this result can be extended to scenarios where data arrivals follow a Markov process.

Corollary 1. For the AoI function defined in (7), the time-average cost $\mathcal{C}(s_0, \pi)$ is bounded under the proposed scheduling policy $\tilde{\pi}^*$ if and only if the following condition is satisfied:

$$\rho(\Omega(I - \lambda_i \mathcal{P}_i)) < \frac{1}{e^r}, \forall i \in \mathcal{N}. \quad (22)$$

In the following, we consider a more complex case where the data arrival process evolves under a Markov chain. Assume

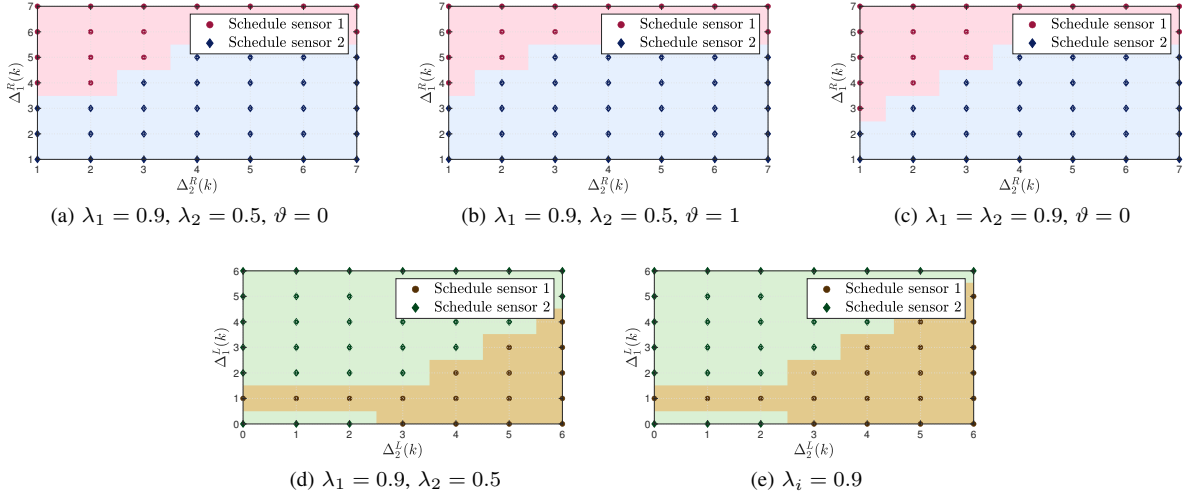


Fig. 4. Scheduling structure of SISP in the two sensor system under different cases.

that the probability of no data arrival at the current time slot is $\tilde{\lambda}_i$ when no data arrived in the previous time slot, i.e., $\Pr\{\gamma_i^L(k) = 0 | \gamma_i^L(k-1) = 0\} = \tilde{\lambda}_i$. When data arrived in the previous time slot, the probability of data arrival at the current time slot is set as $\bar{\lambda}_i$, i.e., $\Pr\{\gamma_i^L(k) = 1 | \gamma_i^L(k-1) = 1\} = \bar{\lambda}_i$. We can get a new corollary of Theorem 4.

Corollary 2. For the AoI function defined in (8), when the data arrival is a Markov process with transition matrix $\begin{bmatrix} \tilde{\lambda}_i & 1 - \tilde{\lambda}_i \\ 1 - \bar{\lambda}_i & \bar{\lambda}_i \end{bmatrix}$, the time-average cost $\mathcal{C}(s_0, \pi)$ is bounded under the proposed scheduling policy $\hat{\pi}^*$ if and only if the following condition is satisfied:

$$\rho(\Omega(I - \hat{\lambda}_i \mathcal{P}_i)) < \frac{1}{\rho^2(A_i)}, \forall i \in \mathcal{N}, \quad (23)$$

where $\hat{\lambda}_i = \min\{1 - \tilde{\lambda}_i, \bar{\lambda}_i\}$.

Proof. See Appendix F. \square

V. SIMULATION STUDY

To demonstrate the performance of the proposed scheduling strategy, we conduct simulation experiments using the AoI functions provided in Examples 1 and 2. First, in the two-sensor model, we verify the effectiveness of the two-stage AoI mechanism and analyze the scheduling structure. Then, in the more complex multi-sensor model, we further validate the superiority of Algorithm 1 through comparative experiments.

A. Demonstration of State Evolution and Scheduling Structure

To provide more general results, we adopt the AoI function (8) from Example 2 as the model for the wireless monitoring networks. The system parameters are considered as follows:

$$A_i = \begin{bmatrix} 1.1 & 0.5 \\ 0 & 0.2 \end{bmatrix}, C_i = \begin{bmatrix} 1 & 1 \end{bmatrix}, \Sigma_i^\omega = \begin{bmatrix} 1 & 0 \\ 0 & 1 \end{bmatrix},$$

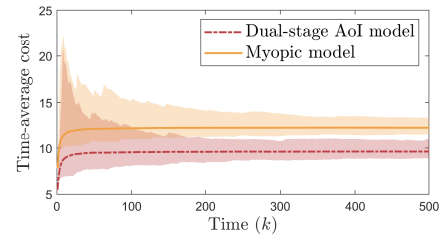
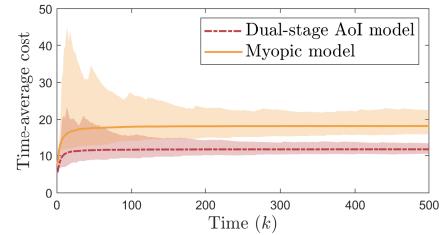

 (a) $\lambda_1 = \lambda_2 = 0.9$.

 (b) $\lambda_1 = 0.9, \lambda_2 = 0.5$.

Fig. 5. Comparison of the time-average cost for myopic model and dual-stage AoI model.

and the covariance of measurement noise is 0.8. Then, the steady-state error covariance \bar{P}_i is computed as

$$\bar{P}_i = \begin{bmatrix} 0.9038 & -0.5175 \\ -0.5175 & 0.7464 \end{bmatrix}.$$

For the two-state memory-based channel model, we suppose the successful transmission probability as $p_i^0 = 0.5$ for bad state and $p_i^1 = 1$ for good state, respectively. The transition probabilities as set as $\kappa_{00} = 0.5, \kappa_{01} = 0.5, \kappa_{10} = 0.2, \kappa_{11} = 0.8$, reflecting a fading channel scenario typical in industrial mobility environments. In order to avoid computational complexity growing indefinitely, the state space truncation is given by $\Delta_i^R = 7$. According with the convergence condition in Theorem 4, we first assume that random data arrival rate $\varepsilon_i = 0.9$ for both sensors. The evolution of AoI function $f(\Delta_i^R(k))$ is plotted in Fig. 3, where the evolution $\Delta_i^R(k)$ and $\Delta_i^L(k)$ are also given.

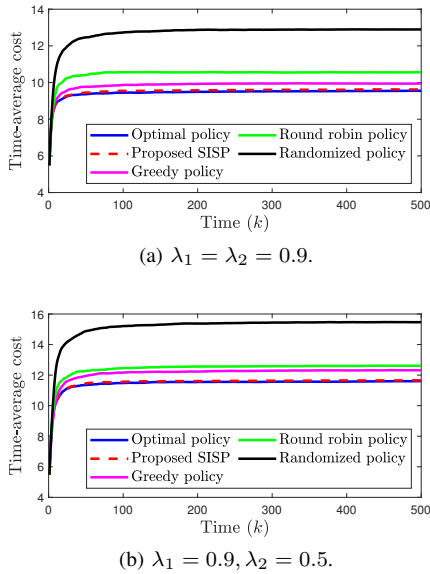


Fig. 6. Performance comparison of different scheduling policies for AoI function in Example 2.

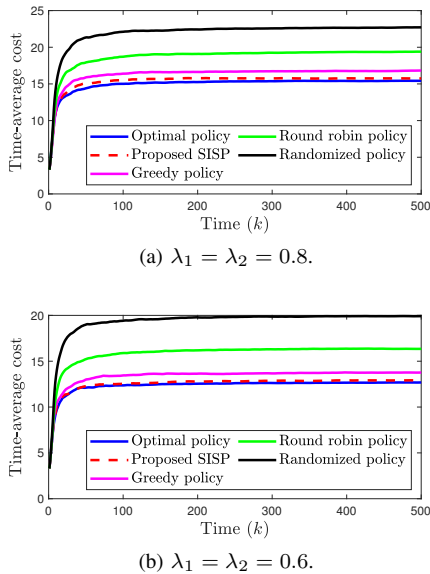


Fig. 7. Performance comparison of different scheduling policies for AoI function in Example 1.

In order to reveal the dynamic properties of different arrival rates, we define $\lambda_1 = \lambda_2 = 0.9$ in Fig. 3a and 3b, and $\lambda_2 = 0.5$ in Fig. 3c, which obviously meets the convergence condition presented in Theorem 4. From Fig. 3a and 3b we can find that the update of AoRI depends on AoLI and its value is updated only when the scheduling is successful, which corresponds to evolution law in Fig. 2. Moreover, the tendency of $f(\Delta_i^R(k))$ is directly related to AoRI and gradually converges to be stable. We then investigate the case where the arrival rate of monitoring data in sensor 2 is $\lambda_2 = 0.5$. It is easy to observe Fig. 3c that the update rate of AoLI is significantly reduced, the value of AoRI does not increase notably due to the proposed scheduling policy.

Next, we continue to use the previously defined parameters

to investigate the scheduling structure. In Fig. 4, we give scheduling results of SISP under different settings of λ_i . As shown in Fig. 4a and 4b, the scheduling results exhibit a threshold structure w.r.t. AoRI under both $\vartheta = 0$ and $\vartheta = 1$, verifying the proposed Theorem 3, where AoLI is fixed as $\Delta_1^L(k) = 7, \Delta_2^L(k) = 6$. For sensor $i \in \{1, 2\}$, the larger the value of $\Delta_i^R(k)$, the more likely the sensor i is to be scheduled. Besides, by comparing Fig. 4a and Fig. 4b, the frequency of scheduling sensor 2 is higher under good channel state because the lower λ_2 makes updates to $\Delta_i^R(k)$ more urgent for maintaining freshness. Similarly, when λ_2 is increased to $\lambda_1 = 0.9$, as shown in Fig. 4c, the frequency of scheduling sensor 2 decreases. Fig. 4d and 4e illustrate the scheduling decisions under different AoLI values, with AoRI fixed at $\Delta_1^R(k) = 2, \Delta_2^R(k) = 3$, which clearly shows that there exists no threshold structure w.r.t. AoLI. The results in Fig. 4d and 4e also confirm that sensor 2 is easier to be scheduled under a relatively lower data arrival rate. In order to display the superiority of the proposed dual-stage AoI model under random data arrivals, we compare the time-average cost with the traditional single-stage AoI model, which neglects the AoLI and is thus called myopic model. Fig. 5 gives the contrast results, it is evident that dual-stage AoI model outperforms myopic model in terms of monitoring performance and stability.

B. Performance Comparison with Different Policies

First, four common scheduling policies are introduced for the comparison. The maximum age first (MAF) policy [16]: Select the sensor with the largest AoRI to transmit in each time slot. The maximum error first (MEF) policy [40]: Select the sensor with the largest error to transmit in each time slot, similar to the greedy policy. The Round-Robin policy [41]: Schedule sensors in turn each time based on the established sequence. The randomized policy: Schedule sensors randomly in certain probabilities, which are considered to be proportional to the information arrival rates of corresponding sensors, i.e., $p_i^R = \vartheta_i / \sum_{j=1}^N \vartheta_j$. For homogeneous systems, the MAF and MEF policies yield identical performance and can be unified into the Greedy policy. In addition, the optimal policy is also considered to demonstrate the near-optimality of SISP. For the AoI function in Example 2, we follow parameter settings in the previous subsection and conduct 500 Monte Carlo simulations, and results are plotted in Fig. 6. It is obvious that SISP outperforms the four other methods significantly with near-optimal performance and the smaller value of ϑ_i explicitly leads to a greater performance gap. It should also be noted that the higher ϑ_i results in lower scheduling costs, which is intuitive, as more frequent updates lead to fresher information. Without loss of generality, we consider the AoI function of Example 1, where r is defined as 0.5 and other settings remain unchanged. Fig. 7 shows the similar comparison results with $\varepsilon_i = 0.8$ and 0.6.

Then, we further examine scheduling performance in a network composed of three heterogeneous systems, where the first system model is the same as previously considered, while the second and third ones are modeled as two-link planar

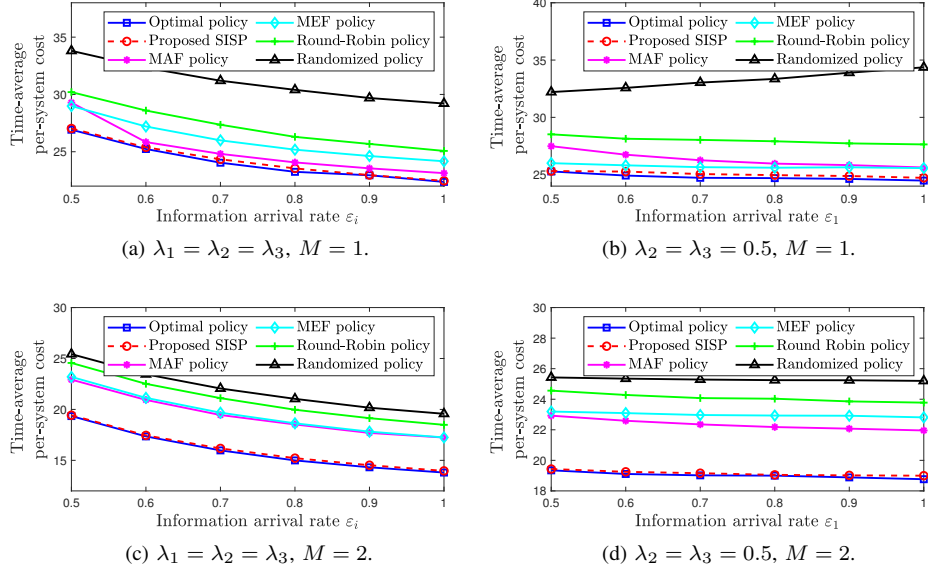


Fig. 8. Performance comparison of different scheduling policies in heterogeneous systems.

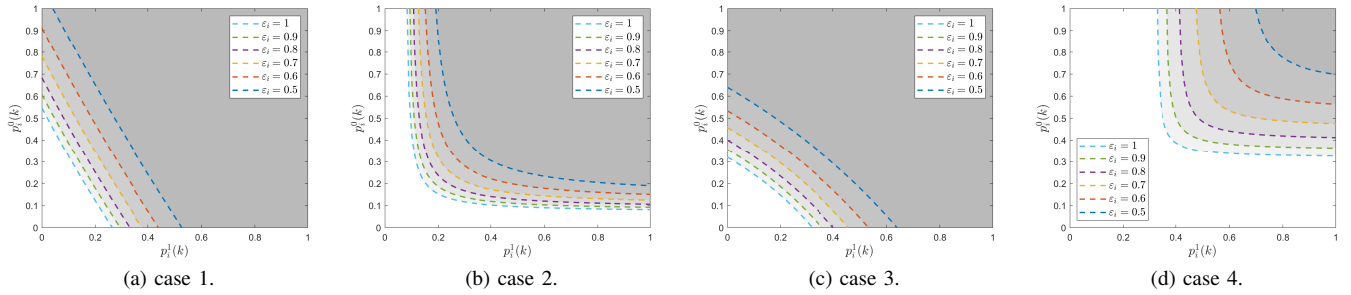


Fig. 9. Feasible region of transmission probabilities for two states under different random arrival rates.

industrial robots with a sampling interval of $15ms$ [42]. The corresponding system parameters are given as follows:

$$A_2 = A_3 = \begin{bmatrix} 1.0058 & 0.0150 & -0.0016 & 0 \\ 0.7808 & 1.0058 & -0.2105 & -0.0016 \\ -0.1160 & 0.0000 & 1.0077 & 0.0150 \\ -0.7962 & -0.0060 & 1.0294 & 1.0077 \end{bmatrix},$$

$$\Sigma_1^\omega = \Sigma_2^\omega = \sigma\sigma^T, \sigma = [0.003 \quad 1 \quad -0.005 \quad -2.15],$$

$$C_1 = C_2 = \begin{bmatrix} 1 & 0 & 0 & 0 \\ 0 & 0 & 1 & 0 \end{bmatrix}.$$

Thus, the steady state of error covariance is computed as

$$\bar{P}_2 = \bar{P}_3 = \begin{bmatrix} 0.0003 & 0.0077 & -0.0002 & -0.0148 \\ 0.0077 & 1.3150 & -0.0130 & -2.8174 \\ -0.0002 & -0.0130 & 0.0007 & 0.0289 \\ -0.0148 & -2.8174 & 0.0289 & 6.0613 \end{bmatrix}.$$

The transmission probabilities of two channel states are supposed as $p_i^0 = 0.4, p_i^1 = 0.9$, and $\kappa_{00} = 0.4, \kappa_{01} = 0.6, \kappa_{10} = 0.3, \kappa_{11} = 0.7$. The influence of various data arrival rates and the number of scheduled sensors on monitoring performance is studied in different policies. All simulations in Fig. 8 shows the time-average per-system cost that our proposed SISP get a good lead in the comparison, and it nearly

achieves performance identical to that of the optimal policy. By comparing results of $m = 1$ and $m = 2$, the performance gap get smaller when more sensors are scheduled. Moreover, compared with the case where all sensors share the same data arrival rate, the performance varies more smoothly when only one sensor's data arrival rate changes. Specially, when only one sensor is scheduled, the randomized policy even cause the cost to increase as the λ_1 increases, because the AoI function of sensor 1 contributes a small portion to the total cost. This further verifies the practicality of our scheduling policy.

To study the influence of data arrival rates to the feasible region of channel states when there exist a memory-based channel, we present several sets of results in Fig. 9 illustrating the relationship between λ_i and p_i^j . According to Theorem 4, the feasible value of p_i^j is affected by $\rho(A_i)$. For case 1, we set $\rho(A_i) = 1.1$, and $\kappa_{00} = 0.4, \kappa_{01} = 0.6, \kappa_{10} = 0.3, \kappa_{11} = 0.7$. As shown in Fig. 9a, the feasible region becomes smaller as the decrease of λ_i . Then, we adjust transition probabilities of channel states in case 2, that is $\kappa_{00} = 0.9, \kappa_{01} = 0.1, \kappa_{10} = 0.1, \kappa_{11} = 0.9$, and results are provided in Fig. 9b. In this case, the channel tends to remain in its previous state, i.e., the channel memory becomes stronger, and thus the feasible region of p_i^j value shrinks significantly. Utilizing Corollary

1, the AoI function (7) is also considered with $r = 0.5$ and it derives a smaller region due to $e^r > \rho^2(A_i)$, which is plotted in Fig. 9d. On the contrary, the region becomes larger when transition probabilities are changed to case 3 with $\kappa_{00} = 0.2, \kappa_{01} = 0.8, \kappa_{10} = 0.8, \kappa_{11} = 0.2$, given in Fig. 9c. It means that more frequent state switching will lead to more feasible value of p_i^j .

VI. CONCLUSION

In this paper, we addressed the transmission scheduling problem for optimizing the AoI function modeled based on monitoring performance, where monitoring data arrives randomly and channel state exhibits temporal correlation. We formulated a dual-AoI model to describe different evolution stages, and derived a low-complexity scheduling algorithm based on the structural properties of the MDP. Theoretical analysis revealed that the optimal policy follows a channel state-dependent threshold structure w.r.t. AoRI and established the necessary and sufficient condition for monitoring stability. Results of simulations demonstrate that the proposed policy significantly outperforms existing baselines. Specially, dual-stage AoI model is more effective compared with single-stage model for random data arrivals. Notably, we observe that the threshold structure applies only to AoRI, and sensors with higher arrival rates are prioritized. Furthermore, higher data arrival rates effectively expand the stability region, allowing the system to tolerate lower channel qualities. Future research will focus on extending our conclusions to multi-hop networks and incorporating learning-based methods to design intelligent scheduling methods for control aware communication.

APPENDIX A PROOF OF THEOREM 1

To confirm the existence of deterministic stationary policy for the Problem 2, we should verify the conditions proposed in [43, Theorem 2], listed as follows:

- 1) There exists a stationary policy π inducing an irreducible positive recurrent Markov chain such that the average cost $\mathcal{C}(s_0, \pi)$ is bounded.
- 2) For any positive number r , the set $\{s | c(s, \pi) < r\}$ is finite.

According to the formulated optimization problem, the action space is finite and the one-step cost is bounded below by 0. Besides, if we suppose that there exists a policy π with the bounded average cost, such that

$$\lim_{T \rightarrow \infty} \frac{1}{T} \sum_{k=1}^T \mathbb{E}[c(s(k), d(k))] < \infty. \quad (24)$$

Therefore, the condition 1) holds. The AoI function $f(\Delta_i^R(k))$ considered in this paper is nondecreasing with Δ_i^R , thus the number of s is finite for $c(s, \pi) < r$ when $r > 0$, and the condition 2) is verified. Then, Theorem 1 is proved.

APPENDIX B PROOF OF LEMMA 1

By iterating the action-value function, $Q(s)$ of the $(n+1)$ -th iteration can be described as below for any s :

$$Q_{n+1}(s) = \min_{d \in \mathcal{A}} \Theta_{n+1}(s, d) - \min_{d \in \mathcal{A}} \Theta_{n+1}(s_r, d) \quad (25)$$

where s_r is a definite state. For any initial value of $Q_1(s)$, we have $\lim_{n \rightarrow \infty} Q_n(s) = Q(s)$. The optimal policy of n th iteration is further denoted as $\pi_n^*(s) = \arg \min_{d \in \mathcal{A}} \Theta_{n+1}(s, d)$ from (17), where $\pi_n^*(s) = (\pi_{i,n}^*(s))_{i \in \mathcal{N}}$. Then, we use the mathematical induction to verify Lemma 1.

Given the initialized $Q_1(s)$, assume $Q_1(s^b) \geq V_1(s^a)$ holds, as well as $Q_n(s^b) \geq Q_n(s^a)$. For $(n+1)$ -th iteration, utilizing the form in (25) can derive that for s^a there exists

$$Q_{n+1}(s^a) = \Theta_{n+1}(s^a, \pi_n^*(s^a)) - \Theta_{n+1}(s_r, \pi_n^*(s_r)), \quad (26)$$

which can infer the following inequality via the policy optimality

$$\begin{aligned} Q_{n+1}(s^a) &\leq \Theta_{n+1}(s^a, \pi_n^*(s^b)) - \Theta_{n+1}(s_r, \pi_n^*(s_r)) \\ &= c(s^a, \pi_n^*(s^b)) + \sum_{s^{a'} \in \mathcal{S}} \Pr\{s^{a'} | s^a, \pi_n^*(s^b)\} Q_n(s^{a'}) \\ &\quad - \Theta_{n+1}(s_r, \pi_n^*(s_r)). \end{aligned} \quad (27)$$

Similarly, for state s^b we can get $Q_{n+1}(s^b) = c(s^b, \pi_n^*(s^b)) + \sum_{s^{b'} \in \mathcal{S}} \Pr\{s^{b'} | s^b, \pi_n^*(s^b)\} Q_n(s^{b'}) - \Theta_{n+1}(s_r, \pi_n^*(s_r))$. Note that for each sensor of state s^b there exist two possible actions: $\pi_{i,n}^*(s^b) = 0$ and $\pi_{i,n}^*(s^b) = 1$. Regardless of which case, both $\tilde{\Delta}_i^{L,b} \geq \tilde{\Delta}_i^{L,a}$ and $\tilde{\Delta}_i^{R,b} \geq \tilde{\Delta}_i^{R,a}$ hold, leading us to conclude that

$$\begin{aligned} &\sum_{s^{a'} \in \mathcal{S}} \Pr\{s^{a'} | s^a, \pi_n^*(s^b)\} Q_n(s^{a'}) \\ &\leq \sum_{s^{b'} \in \mathcal{S}} \Pr\{s^{b'} | s^b, \pi_n^*(s^b)\} Q_n(s^{b'}), \end{aligned} \quad (28)$$

which can deduce inequality $Q_{n+1}(s^a) \leq Q_{n+1}(s^b)$ for $n > 1$ via induction. Furthermore, due to the convergence of $Q_n(s)$, we can prove the inference of Lemma 1.

APPENDIX C PROOF OF THEOREM 2

In order to prove the existence of distributed structure, we first introduce the randomized policy π_R . Under the randomized policy π_R , the i -th sensor is scheduled with a certain probability p_i^R , such that the Bellman equation similar to (16) is established as follows:

$$\phi^\dagger + Q^R(s) = c^\dagger(s, d) + \sum_{s' \in \mathcal{S}} \mathbb{E}^{\pi_R}[\Pr\{s' | s, d\}] Q^R(s'), \quad (29)$$

where ϕ^\dagger is the cost value under policy π_R and $Q^R(s)$ is the corresponding value function. Then, the decomposition property of $Q^R(s)$ will be proved. According to the result in Theorem 1, the policy π^R is an unichain policy, such that the solution of (29) also exists. Depending on the the relationship

between the joint distribution and the marginal distribution, for any state $s \in \mathcal{S}$ we have

$$\begin{aligned}
 \sum_{s' \in \mathcal{S}} \Pr\{s' | s, d\} &= \sum_{s' \in \mathcal{S}} \Pr\{(s^\Delta)', \vartheta' | s^\Delta, \vartheta, d\} \\
 &= \sum_{s'_i \in \mathcal{S}_i} \Pr\{(s_i^\Delta)', \vartheta' | s_i^\Delta, \vartheta, d\} \\
 &= \sum_{s'_i \in \mathcal{S}_i} \Pr\{(s_i^\Delta)', \vartheta' | s_i^\Delta, \vartheta, d_i\}, \tag{30}
 \end{aligned}$$

where s_i is defined as (s_i^Δ, ϑ) and its corresponding state space is \mathcal{S}_i . Hence, it is obvious that $\sum_{s' \in \mathcal{S}} \Pr\{s' | s, d\} = \sum_{s'_i \in \mathcal{S}_i} \Pr\{s' | s_i, d_i\}$. Combined with $\phi^\dagger = \sum_{i \in \mathcal{N}} \phi_i^\dagger$ and $Q^R(s) = \sum_{i \in \mathcal{N}} Q_i^R(s_i)$, there exists following Bellman equation for the i -th sensor:

$$\begin{aligned}
 \phi_i^\dagger + Q_i^R(s_i) &= c_i^\dagger(s_i, d_i) \\
 &+ \sum_{s'_i \in \mathcal{S}_i} \mathbb{E}^{\pi^R}[\Pr\{s'_i | s_i, d_i\}] Q_i^R(s'_i), \tag{31}
 \end{aligned}$$

where $\Pr\{s'_i | s_i, d_i\}$ can be computed from (11), $c_i^\dagger(s_i, d_i) = \mathbb{E}[c_i(s_i, d_i)] = f(\Delta_i^R)$, ϕ_i^\dagger denotes the optimal cost of the i -th sensor and $Q_i^R(s_i)$ is the corresponding value function. Then, by the concept of approximate dynamic programming [38], the value function given in (16) is approximated to $Q^R(s)$ that equal to $\sum_{i \in \mathcal{N}} Q_i^R(s_i)$, and we can further obtain the form of structure-informed scheduling policy $\tilde{\pi}^*$.

Next, we will prove that the long-term time-average cost under $\tilde{\pi}^*$ is lower than under randomized policy π^R . Applying the proof of [37, Proposition 4.4.2], we express the performance of various policies as the gain-bias form. As policy π^R is an unichain policy, define the gain of π^R as a scalar ψ^R , and its bias is denoted as a vector ν^R for long-term. Then, the simplified form of Bellman equation is written as follows:

$$\psi^R \mathbf{1} + \nu^R = \mathcal{T}^R \nu^R, \tag{32}$$

where \mathcal{T}^R is the Bellman operator and $\mathbf{1}$ denotes a vector where all elements are 1. For the proposed structure-informed policy $\tilde{\pi}^*$, the unichain cannot be guaranteed, such that the gain is defined as a vector ψ^\dagger and the corresponding bias is ν^\dagger , the Bellman equation is given by $\psi^\dagger + \nu^\dagger = \mathcal{T}^\dagger \nu^\dagger$, where \mathcal{T}^\dagger is the Bellman operator of $\tilde{\pi}^*$ with one-step cost vector c^\dagger . Due to the invariance of ψ^\dagger under state transitions in long-term, we have $\psi^\dagger = P^\dagger \psi^\dagger$, where P^\dagger is the transition probability matrix.

In order to show the performance difference after applying policy $\tilde{\pi}^*$, we denote it by $\mu = \psi^R \mathbf{1} + \nu^R - \mathcal{T}^\dagger \nu^R$. Then, substituting (32) and \mathcal{T}^\dagger into μ we have

$$\begin{aligned}
 \mu &= \psi^R \mathbf{1} + \nu^R - (c^\dagger + P^\dagger \nu^R) \\
 &= \psi^R \mathbf{1} - \psi^\dagger + \nu^R - \nu^\dagger + \psi^\dagger + \nu^R - (c^\dagger + P^\dagger \nu^R) \\
 &= \psi^R \mathbf{1} - \psi^\dagger + \Upsilon - P^\dagger \Upsilon. \tag{33}
 \end{aligned}$$

By multiplying both sides of (33) by P^\dagger and iteratively summing L steps, we can obtain

$$\begin{aligned}
 &\lim_{L \rightarrow \infty} \frac{1}{L} \sum_{l=0}^{L-1} (P^\dagger)^l \mu \\
 &= \lim_{L \rightarrow \infty} \frac{1}{L} \sum_{l=0}^{L-1} (P^\dagger)^l (\psi^R \mathbf{1} - \psi^\dagger + \Upsilon - P^\dagger \Upsilon) \\
 &= \lim_{L \rightarrow \infty} \frac{1}{L} \sum_{l=0}^{L-1} (P^\dagger)^l (\psi^R \mathbf{1} - \psi^\dagger) \\
 &\quad + \lim_{L \rightarrow \infty} \frac{1}{L} \sum_{l=0}^{L-1} (P^\dagger)^l (I - P^\dagger) \Upsilon \\
 &= \lim_{L \rightarrow \infty} \frac{1}{L} [L(\psi^R \mathbf{1} - \psi^\dagger) + (I - (P^\dagger)^L) \Upsilon] \\
 &= \psi^R \mathbf{1} - \psi^\dagger. \tag{34}
 \end{aligned}$$

Then, it is easy to get $\lim_{L \rightarrow \infty} \frac{1}{L} \sum_{l=0}^{L-1} (P^\dagger)^l \mu = \bar{P}^\dagger \mu = \psi^R \mathbf{1} - \psi^\dagger$, where \bar{P}^\dagger is the convergence of P^\dagger . Recall the MDP definition [37, Proposition 5.4.2], there must exists $\Pr\{s' | s, d^a\} \neq \Pr\{s' | s, d^b\}$ under the assumption of $d^a \neq d^b$, resulting in $\mu > 0$. Hence, $\psi^R \mathbf{1} > \psi^\dagger$, thus the proposed scheduling policy performs better than the randomized policy in theory. The proof is accomplished.

APPENDIX D PROOF OF THEOREM 3

To verify the threshold structure, we should first demonstrate the monotonicity of the decomposed value function $Q_i^R(s_i)$ based on Lemma 1. Similar to (18), under randomized policy π^R , the single action-value function of the n th step iteration can be described as $\Theta_n^\dagger(s_i) = c_i(s_i, d_i) + \sum_{s'_i \in \mathcal{S}_i} \mathbb{E}^{\pi^R}[\Pr\{s'_i | s_i, d_i\}] Q_{i,n}^R(s'_i)$. $Q_{i,n}^R(s_i)$, like (25), is iterated by $\Theta_n^\dagger(s_i) - \Theta_n^\dagger(s_i^r)$ with the definite state s_i^r . For the supposed states s_i^a and s_i^b with $\Delta_i^{L,a} \leq \Delta_i^{L,b}$, $\Delta_i^{R,a} \leq \Delta_i^{R,b}$ under a certain channel state, one has

$$Q_{i,n}^R(s_i^a) \leq Q_{i,n}^R(s_i^b), \tag{35}$$

which can further deduce the monotonicity of $Q_i^R(s_i)$ according to the convergence of $Q_{i,n}^R(s_i)$.

Next, the submodularity of $\Theta^\dagger(s, d)$ will be proved to show the threshold property, such that for s^a, s^b with $\tilde{\Delta}^{L,a} = \tilde{\Delta}^{L,b}$ there exists $d_i = 1$ when $\Delta_i^{R,a} \geq \Delta_i^{R,b}$. Besides, $\Theta^\dagger(s^a, d) - \Theta^\dagger(s^a, d') \leq \Theta^\dagger(s^b, d) - \Theta^\dagger(s^b, d')$ holds for $\forall i \in \mathcal{N}$. By the definition of $\Theta^\dagger(s, d)$, for any s^a, s^b we have

$$\begin{aligned}
 &\Theta^\dagger(s^a, d) - \Theta^\dagger(s^a, d') - \Theta^\dagger(s^b, d) + \Theta^\dagger(s^b, d') \\
 &\stackrel{(a)}{=} \sum_{s^a \in \mathcal{S}} \Pr\{s_d^a | s^a, d\} Q^R(s_d^a) - \sum_{s^a \in \mathcal{S}} \Pr\{s_d^a | s^a, d'\} Q^R(s_d^a) \\
 &\quad - \sum_{s^b \in \mathcal{S}} \Pr\{s_d^b | s^b, d\} Q^R(s_d^b) + \sum_{s^b \in \mathcal{S}} \Pr\{s_d^b | s^b, d'\} Q^R(s_d^b) \\
 &\stackrel{(b)}{=} \sum_{s^b \in \mathcal{S}} \Pr\{s_d^b | s^b, d'\} Q^R(s_d^b) \\
 &\quad - \sum_{s^a \in \mathcal{S}} \Pr\{s_d^a | s^a, d'\} Q^R(s_d^a), \tag{36}
 \end{aligned}$$

where the only difference of s^a and s^b is the AoFI that corresponding sensor is scheduled, i.e. $\Delta_i^{R,a} \geq \Delta_i^{R,b}$ for

$d_i = 1$. Hence, the same states will be reached from s^a and s^b under the action d , by which (a) is deduced to (b) in (36). For two terms in (b), considering the situation of sensor i , $i \in \mathcal{N}^+ \triangleq \{i | d_i = 1, i \in N\}$, because $s_{d'}^a = s_{d'}^b$ for other sensors. Then, for the case of $d_i' = 0$, there exists $s_{i,d'}^a = (\Delta_i^{L,a}, \Delta_i^{R,a} + 1, \vartheta)$, $s_{i,d'}^b = (\Delta_i^{L,b}, \Delta_i^{R,b} + 1, \vartheta)$. It is obvious that $\tilde{\Delta}^{L,a} \geq \tilde{\Delta}^{L,b}$, $\tilde{\Delta}^{R,a} \geq \tilde{\Delta}^{R,b}$ under this case, such that the RHS of (36) is negative and the following inequality holds:

$$\Theta^\dagger(s^a, d) - \Theta^\dagger(s^a, d') \leq \Theta^\dagger(s^b, d) - \Theta^\dagger(s^b, d'). \quad (37)$$

From (20), it is known that $\Theta^\dagger(s, d) \leq \Theta^\dagger(s, d')$ for $d \neq d'$, so $\tilde{\pi}^*(s) = d$. Assume that for state s' there exists $\Delta_i^{R'} \geq \Delta_i^R$ with $\tilde{\Delta}^L = \tilde{\Delta}^{L'}$, and $\Theta^\dagger(s', d) \leq \Theta^\dagger(s', d')$ holds for $d \in \mathcal{A}$, $d \neq d'$ if Theorem 3 is right. According to the result of (37), we can obtain $\Theta^\dagger(s', d) - \Theta^\dagger(s', d') \leq \Theta^\dagger(s, d) - \Theta^\dagger(s, d')$, thus $\tilde{\pi}^*(s) = \tilde{\pi}^*(s') = d$. The proof is completed accordingly.

APPENDIX E PROOF OF THEOREM 4

Define ξ_{s_i} as the limiting distribution of state s_i , which is constrained by the proposed scheduling policy. According to the structured property of policy $\tilde{\pi}^*$, $d_i = 1$ when AoRI $\Delta_i^R \geq \Delta_i^{R*}$ under a certain channel state ϑ . Define the initial state as $s_{i,0} = (0, 1, 0)$. As the Markov chain s_i is irreducible, aperiodic and recurrent for policy $\tilde{\pi}^*$, such that any state has a positive probability to reach all states and the expectation time of the first time revisiting state $s_{i,0}$ is bounded, leading to the existence of unique limiting distribution of state s_i . Denote by $\bar{\Delta}_i^{R*}$ the maximum AoRI under $\vartheta = 0$ and $\vartheta = 1$ as $\max\{\Delta_i^{R*} | \vartheta \in \{0, 1\}\}$, and then we consider the following cases for limiting distribution ξ_{s_i} :

- 1) For the case of $0 < \Delta_i^R \leq \bar{\Delta}_i^{R*}$, if $\Delta_i^{R'} = \Delta_i^R + 1$, then we have

$$\xi_{s_i'} = \sum_{\vartheta \in \{0, 1\}} \xi_{s_i} \Pr\{s_i' | s_i, \tilde{\pi}^*\}. \quad (38)$$

When $\Delta_i^R \leq \Delta_i^{R*}$, then the value of $\Pr\{s_i' | s_i, \tilde{\pi}^*\}$ is $\lambda_i \kappa_{\vartheta\vartheta'}$ for $\Delta_i^{L'} = 0$ or $(1 - \lambda_i) \kappa_{\vartheta\vartheta'}$ for $\Delta_i^{L'} = \Delta_i^L + 1$. When $\Delta_i^R > \Delta_i^{R*}$, the corresponding situation is no data arrival or transmission failure, then the value of $\Pr\{s_i' | s_i, \tilde{\pi}^*\}$ is given as $\kappa_{\vartheta\vartheta'}(1 - \lambda_i p_i^{\vartheta'}(k))$.

- 2) For the case of $\Delta_i^R > \bar{\Delta}_i^{R*}$, the value of $\Pr\{s_i' | s_i, \tilde{\pi}^*\}$ can refer to the second situation in case 1, such that $\Pr\{s_i' | s_i, \tilde{\pi}^*\} = \kappa_{\vartheta\vartheta'}(1 - \lambda_i p_i^{\vartheta'}(k))$.

It is obvious that $\mathcal{C}(s_0, \pi)$ is bounded under case 1) due to $\Delta_i^R \leq \bar{\Delta}_i^{R*}$, but case 2) with $\Delta_i^R > \bar{\Delta}_i^{R*}$ cannot guarantee the cost boundness. We expand $\xi_{s_i'}$ of case 2) based on two different channel states and obtain the following form:

$$\begin{aligned} \xi_{s_i'(\vartheta'=0)} &= \xi_{s_i(\vartheta=0)} \kappa_{00}(1 - \lambda_i p_i^0(k)) \\ &\quad + \xi_{s_i(\vartheta=1)} \kappa_{10}(1 - \lambda_i p_i^0(k)), \\ \xi_{s_i'(\vartheta'=1)} &= \xi_{s_i(\vartheta=0)} \kappa_{01}(1 - \lambda_i p_i^1(k)) \\ &\quad + \xi_{s_i(\vartheta=1)} \kappa_{11}(1 - \lambda_i p_i^1(k)). \end{aligned} \quad (39)$$

In order to simplify the presentation, we define $\xi_{s_i} = (\xi_{s_i(\vartheta=0)}, \xi_{s_i(\vartheta=1)})$. According to the form of (39), it can be

further expressed as $\xi_{s_i'} = \xi_{s_i} \Omega(I - \lambda_i \mathcal{P}_i)$. After continuous iterations, we get when AoRI evolves to $(\bar{\Delta}_i^{R*} + \tau)$, $\tau \in \mathbb{N}^+$,

$$\xi_{s_i(\bar{\Delta}_i^{R*} + \tau)} = \xi_{s_i(\bar{\Delta}_i^{R*})} (\Omega(I - \lambda_i \mathcal{P}_i))^\tau. \quad (40)$$

According to the AoI function proposed in (8), the convergence of time-average monitoring cost $\mathcal{C}(s_0, \pi)$ is directly related to $h^{\Delta_i^R}(\bar{P}_i)$. Hence, we have the following equation based on the limiting distribution concept:

$$\mathcal{E} = \sum_{i=1}^N \sum_{\Delta_i^R=1}^{\infty} \tilde{\xi}_{s_i(\Delta_i^R)} h^{\Delta_i^R}(\bar{P}_i), \quad (41)$$

where $h(\bar{P}_i) \triangleq A_i \bar{P}_i A_i^T + \Sigma_i^\omega$, $\tilde{\xi}_{s_i(\Delta_i^R)} \triangleq \sum_{\vartheta \in \{0, 1\}} \xi_{s_i(\Delta_i^R, \vartheta)} = \|\xi_{s_i(\Delta_i^R)}\|_1$ and $\sum_{\Delta_i^R=1}^{\infty} \tilde{\xi}_{s_i(\Delta_i^R)} = 1$. By the definition of $h(\bar{P}_i)$, $h^{\Delta_i^R}(\bar{P}_i)$ is monotone non-decreasing such that $E < \infty$ can ensure the boundedness of time-average cost, so as to the stability of monitoring performance. Using the matrix theory, the eigenvalue of nonnegative matrix $\Omega(I - \lambda_i \mathcal{P}_i)$ as $\rho(\Omega(I - \lambda_i \mathcal{P}_i))$, thus there exists a eigenvector ε_i satisfying $\rho(\Omega(I - \lambda_i \mathcal{P}_i)) \varepsilon_i = (\Omega(I - \lambda_i \mathcal{P}_i)) \varepsilon_i$. Then, it is easy to get $\xi_{s_i(\bar{\Delta}_i^{R*} + \tau)} \varepsilon_i = \xi_{s_i(\bar{\Delta}_i^{R*})} \rho^\tau (\Omega(I - \lambda_i \mathcal{P}_i)) \varepsilon_i$. There must exist a constant e_τ that $\|\xi_{s_i(\bar{\Delta}_i^{R*} + \tau)}\|_1 = e_\tau \rho^\tau (\Omega(I - \lambda_i \mathcal{P}_i)) \|\xi_{s_i(\bar{\Delta}_i^{R*})}\|_1$. Set $\zeta_i = \sum_{\Delta_i^R=\bar{\Delta}_i^{R*}}^{\infty} \rho^{\Delta_i^R - \bar{\Delta}_i^{R*}} (\Omega(I - \lambda_i \mathcal{P}_i)) \|\xi_{s_i(\bar{\Delta}_i^{R*})}\|_1 h^{\Delta_i^R}(\bar{P}_i)$, we obtain the upper boundness of (41) as $\mathcal{E} \leq \sum_{i=1}^N \bar{e}_\tau \zeta_i$

$$\mathcal{E} \leq \sum_{i=1}^N \bar{e}_\tau \zeta_i, \quad (42)$$

where $\bar{e}_\tau = \max_{\tau \in \mathbb{N}} \{e_\tau\}$ can guarantee the validity of (42). With the whole form of $h(\bar{P}_i)$, ζ_i is expanded as follows:

$$\begin{aligned} \zeta_i &= \sum_{j=\bar{\Delta}_i^{R*}}^{\infty} \rho^{j-\bar{\Delta}_i^{R*}} (\Omega(I - \lambda_i \mathcal{P}_i)) \|\xi_{s_i(\bar{\Delta}_i^{R*})}\|_1 h^j(\bar{P}_i) \\ &= \sum_{j=\bar{\Delta}_i^{R*}}^{\infty} \rho^{j-\bar{\Delta}_i^{R*}} (\Omega(I - \lambda_i \mathcal{P}_i)) \|\xi_{s_i(\bar{\Delta}_i^{R*})}\|_1 \\ &\quad \times \left(A_i^j \bar{P}_i (A_i^T)^j + \sum_{l=0}^{j-1} A_i^l \Sigma_i^\omega (A_i^T)^l \right) \\ &= \|\xi_{s_i(\bar{\Delta}_i^{R*})}\|_1 A_i^{\bar{\Delta}_i^{R*}} \left(\sum_{l=0}^{\infty} \varsigma_{1,i}(l) \right) (A_i^T)^{\bar{\Delta}_i^{R*}} \\ &\quad + \|\xi_{s_i(\bar{\Delta}_i^{R*})}\|_1 \frac{1}{\varsigma_{3,i}} \sum_{l=\bar{\Delta}_i^{R*}-1}^{\infty} \varsigma_{2,i}(l), \end{aligned} \quad (43)$$

where $\varsigma_{1,i}(l) = \rho^l (\Omega(I - \lambda_i \mathcal{P}_i)) A_i^l \bar{P}_i (A_i^T)^l$, $\varsigma_{2,i}(l) = \rho^l (\Omega(I - \lambda_i \mathcal{P}_i)) A_i^l \Sigma_i^\omega (A_i^T)^l$ and $\varsigma_{3,i} = \rho^{\bar{\Delta}_i^{R*}-1} (\Omega(I - \lambda_i \mathcal{P}_i))$. By expanding [44, Lemma 3], ζ_i is surely bounded if and only if $\rho(\Omega(I - \lambda_i \mathcal{P}_i)) < \frac{1}{\rho^2(A_i)}$ holds. Therefore, $\mathcal{E} < \infty$ is ensured and the monitoring cost is convergent.

APPENDIX F PROOF OF COROLLARY 2

Considering that the data arrival process follows a Markov chain, the occurrence of current data arrival depends on the

arrival status in the previous time slot. Therefore, we can obtain the state transition of Δ_i^L as follows:

$$\begin{aligned} & \Pr\{\gamma_i^R(k)|\gamma_i^R(k-1)\} \\ &= \begin{cases} \tilde{\lambda}_i, & \text{if } \gamma_i^R(k) = 0, \gamma_i^R(k-1) = 0, \\ 1 - \tilde{\lambda}_i, & \text{if } \gamma_i^R(k) = 1, \gamma_i^R(k-1) = 0, \\ \bar{\lambda}_i, & \text{if } \gamma_i^R(k) = 1, \gamma_i^R(k-1) = 1, \\ 1 - \bar{\lambda}_i, & \text{if } \gamma_i^R(k) = 0, \gamma_i^R(k-1) = 1, \\ 0, & \text{otherwise.} \end{cases} \quad (44) \end{aligned}$$

Then, the state transition of $s_i^\Delta(k)$ defined in (13) is transformed as the following form:

1) For $d_i(k) = 0$, there exists

$$\begin{aligned} & \Pr\{s_i^\Delta(k)|s_i^\Delta(k-1), \vartheta(k-1), d_i(k) = 0\} \\ &= \begin{cases} \tilde{\lambda}_i, & \text{if } \Delta_i^L(k-1) > 0, \\ & s_i^\Delta(k) = (\Delta_i^L(k-1) + 1, \Delta_i^R(k-1) + 1), \\ \bar{\lambda}_i, & \text{if } \Delta_i^L(k-1) = 0, \\ & s_i^\Delta(k) = (0, \Delta_i^R(k-1) + 1), \\ 1 - \tilde{\lambda}_i, & \text{if } \Delta_i^L(k-1) > 0, \\ & s_i^\Delta(k) = (0, \Delta_i^R(k-1) + 1), \\ 1 - \bar{\lambda}_i, & \text{if } \Delta_i^L(k-1) = 0, \\ & s_i^\Delta(k) = (1, \Delta_i^R(k-1) + 1), \\ 0, & \text{otherwise.} \end{cases} \quad (45) \end{aligned}$$

2) For $d_i(k) = 1$, there exists

$$\begin{aligned} & \Pr\{s_i^\Delta(k)|s_i^\Delta(k-1), \vartheta(k-1), d_i(k) = 1\} \\ &= \begin{cases} \tilde{\lambda}_i p_i^\vartheta(k), & \text{if } \Delta_i^L(k-1) > 0, \\ & s_i^\Delta(k) = (\Delta_i^L(k-1) + 1, \\ & \Delta_i^R(k-1) + 1), \\ \bar{\lambda}_i p_i^\vartheta(k), & \text{if } \Delta_i^L(k-1) = 0, \\ & s_i^\Delta(k) = (0, 1), \\ (1 - \tilde{\lambda}_i) p_i^\vartheta(k), & \text{if } \Delta_i^L(k-1) > 0, \\ & s_i^\Delta(k) = (0, \Delta_i^L(k-1) + 1), \\ (1 - \bar{\lambda}_i) p_i^\vartheta(k), & \text{if } \Delta_i^L(k-1) = 0, \\ & s_i^\Delta(k) = (1, 1), \\ \tilde{\lambda}_i (1 - p_i^\vartheta(k)), & \text{if } \Delta_i^L(k-1) > 0, \\ & s_i^\Delta(k) = (\Delta_i^L(k-1) + 1, \\ & \Delta_i^R(k-1) + 1), \\ \bar{\lambda}_i (1 - p_i^\vartheta(k)), & \text{if } \Delta_i^L(k-1) = 0, \\ & s_i^\Delta(k) = (0, 1), \\ (1 - \tilde{\lambda}_i) (1 - p_i^\vartheta(k)), & \text{if } \Delta_i^L(k-1) > 0, \\ & s_i^\Delta(k) = (0, \Delta_i^R(k-1) + 1), \\ (1 - \bar{\lambda}_i) (1 - p_i^\vartheta(k)), & \text{if } \Delta_i^L(k-1) = 0, \\ & s_i^\Delta(k) = (1, \Delta_i^R(k-1) + 1), \\ 0, & \text{otherwise.} \end{cases} \quad (46) \end{aligned}$$

Referring to the proof of Theorem 4, the boundness of $\mathcal{C}(s_0, \pi)$ cannot be surely bounded when $\Delta_i^R > \bar{\Delta}_i^{R*}$. Then, similar

to (39), we can obtain the distribution of $\xi_{s_i^\Delta}$ under different arrival situations. According to (44), we have following cases:

$$\begin{aligned} & \xi_{s_i^\Delta(\vartheta'=0)} \\ &= \begin{cases} \xi_{s_i(\vartheta=0)} \kappa_{00} (1 - (1 - \tilde{\lambda}_i) p_i^0(k)) \\ + \xi_{s_i(\vartheta=1)} \kappa_{10} (1 - (1 - \tilde{\lambda}_i) p_i^0(k)), & \text{if } \gamma_i^R(k-1) = 0, \\ \xi_{s_i(\vartheta=0)} \kappa_{00} (1 - \bar{\lambda}_i p_i^0(k)) \\ + \xi_{s_i(\vartheta=1)} \kappa_{10} (1 - \bar{\lambda}_i p_i^0(k)), & \text{if } \gamma_i^R(k-1) = 1. \end{cases} \quad (47) \end{aligned}$$

$$\begin{aligned} & \xi_{s_i^\Delta(\vartheta'=1)} \\ &= \begin{cases} \xi_{s_i(\vartheta=0)} \kappa_{01} (1 - (1 - \tilde{\lambda}_i) p_i^1(k)) \\ + \xi_{s_i(\vartheta=1)} \kappa_{11} (1 - (1 - \tilde{\lambda}_i) p_i^1(k)), & \text{if } \gamma_i^R(k-1) = 0, \\ \xi_{s_i(\vartheta=0)} \kappa_{01} (1 - (1 - \bar{\lambda}_i) p_i^1(k)) \\ + \xi_{s_i(\vartheta=1)} \kappa_{11} (1 - (1 - \bar{\lambda}_i) p_i^1(k)), & \text{if } \gamma_i^R(k-1) = 1. \end{cases} \quad (48) \end{aligned}$$

Due to the fact that $\gamma_i^R(k-1)$ has two possible states, $\xi_{s_i^\Delta(\vartheta'=0)}$ and $\xi_{s_i^\Delta(\vartheta'=1)}$ can be discussed separately. Based on the forms of (47) and (48), the original expression in (40) is thus derived in two corresponding cases as follows:

$$\begin{aligned} & \xi_{s_i(\bar{\Delta}_i^{R*} + \tau)} \\ &= \begin{cases} \xi_{s_i(\bar{\Delta}_i^{R*})} (\Omega(I - (1 - \tilde{\lambda}_i) \mathcal{P}_i))^\tau, & \text{if } \gamma_i^R(k-1) = 0, \\ \xi_{s_i(\bar{\Delta}_i^{R*})} (\Omega(I - \tilde{\lambda}_i \mathcal{P}_i))^\tau, & \text{if } \gamma_i^R(k-1) = 1. \end{cases} \quad (49) \end{aligned}$$

And the remaining proof steps follow the same procedure as in (41)-(43). To ensure the convergence of the monitoring cost, both $\rho(\Omega(I - (1 - \tilde{\lambda}_i) \mathcal{P}_i)) < \frac{1}{\rho^2(\bar{A}_i)}$ and $\rho(\Omega(I - \tilde{\lambda}_i \mathcal{P}_i)) < \frac{1}{\rho^2(\bar{A}_i)}$ should be satisfied, such that we can get the stability condition for the Markov arrival process as $\rho(\Omega(I - \hat{\lambda}_i \mathcal{P}_i)) < \frac{1}{\rho^2(\bar{A}_i)}$, where $\hat{\lambda}_i = \min\{1 - \tilde{\lambda}_i, \bar{\lambda}_i\}$. The proof is completed.

REFERENCES

- [1] X. Chen, H. Xing, Q. Zhang, Z. Xiong, Y. Bi, and X. Wang, "Age-of-information-aware hierarchical collaborative inference in digital twin-enabled vehicular edge computing," *IEEE Trans. Netw. Sci. Eng.*, vol. 13, pp. 2388–2404, 2026.
- [2] X. Ling, J. Gong, R. Li, S. Yu, Q. Ma, and X. Chen, "Dynamic age minimization with real-time information preprocessing for edge-assisted IoT devices with energy harvesting," *IEEE Trans. Netw. Sci. Eng.*, vol. 8, no. 3, pp. 2288–2300, 2021.
- [3] K. Liu and J. Zheng, "UAV trajectory optimization for time-constrained data collection in UAV-enabled environmental monitoring systems," *IEEE Internet Things J.*, vol. 9, no. 23, pp. 24 300–24 314, 2022.
- [4] Y. Sun, I. Kadota, R. Talak, and E. Modiano, *Age of information: A new metric for information freshness*. Springer Nature, 2022.
- [5] Y. Qiao, Y. Fu, and M. Yuan, "Communication-control co-design in wireless networks: A cloud control AGV example," *IEEE Internet Things J.*, vol. 10, no. 3, pp. 2346–2359, 2023.
- [6] I. Kadota, A. Sinha, E. Uysal-Biyikoglu, R. Singh, and E. Modiano, "Scheduling policies for minimizing age of information in broadcast wireless networks," *IEEE/ACM Trans. Networking*, vol. 26, no. 6, pp. 2637–2650, 2018.
- [7] X. Xie, T. Zhong, and H. Wang, "Scheduling for maximizing the information freshness in vehicular edge computing-assisted IoT systems," *IEEE Trans. Intell. Transp. Syst.*, vol. 26, no. 3, pp. 4140–4151, 2024.
- [8] F. Zhao, N. Pappas, M. Zhang, and H. H. Yang, "Age of information in random access networks with energy harvesting," *IEEE J. Sel. Areas Commun.*, vol. 43, no. 11, pp. 3813–3829, 2025.

- [9] X. Chen, K. Gatsis, H. Hassani, and S. S. Bidokhti, "Age of information in random access channels," in *IEEE International Symposium on Information Theory (ISIT)*, 2020, pp. 1770–1775.
- [10] I. Kadota and E. Modiano, "Minimizing the age of information in wireless networks with stochastic arrivals," *IEEE Trans. Mobile Comput.*, vol. 20, no. 3, pp. 1173–1185, 2021.
- [11] G. Yao, A. M. Bedewy, and N. B. Shroff, "Age-optimal low-power status update over time-correlated fading channel," *IEEE Trans. Mobile Comput.*, vol. 22, no. 8, pp. 4500–4514, 2022.
- [12] L. Chen and Y. Dong, "Estimating age of information in wireless systems with unknown distributions of inter-arrival/service time," *IEEE Trans. Netw. Sci. Eng.*, vol. 11, no. 6, pp. 6090–6104, 2024.
- [13] R. D. Yates and S. K. Kaul, "The age of information: Real-time status updating by multiple sources," *IEEE Trans. Inf. Theory*, vol. 65, no. 3, pp. 1807–1827, 2018.
- [14] M. A. Abd-Elmagid, H. S. Dhillon, and N. Pappas, "AoI-optimal joint sampling and updating for wireless powered communication systems," *IEEE Trans. Veh. Technol.*, vol. 69, no. 11, pp. 14 110–14 115, 2020.
- [15] W. De Sombre, F. Marques, F. Pyttel, A. Ortiz, and A. Klein, "A unified approach to learn transmission strategies using age-based metrics in point-to-point wireless communication," in *IEEE Global Communications Conference (GLOBECOM)*. IEEE, 2023, pp. 3573–3578.
- [16] T. Zhu, J. Li, H. Gao, Y. Li, and Z. Cai, "AoI minimization data collection scheduling for battery-free wireless sensor networks," *IEEE Trans. Mobile Comput.*, vol. 22, no. 3, pp. 1343–1355, 2023.
- [17] F. Fu, X. Wei, Z. Zhang, L. T. Yang, L. Cai, J. Luo, Z. Zhang, and C. Wang, "Age of information minimization for UAV-assisted internet of things networks: A safe actor-critic with policy distillation approach," *IEEE Trans. Netw. Sci. Eng.*, vol. 11, no. 1, pp. 1265–1276, 2024.
- [18] J. Wang and D. Qiao, "How to minimize the weighted sum AoI in multi-source status update systems: TDMA or NOMA?" *IEEE Trans. Veh. Technol.*, vol. 73, no. 4, pp. 5531–5545, 2023.
- [19] G. Sun, L. Zhang, J. Li, J. Wu, J. Wang, Z. Sun, C. Zhao, and V. C. M. Leung, "Age of information optimization in laser-charged UAV-assisted IoT networks: A multi-agent deep reinforcement learning method," *IEEE Trans. Netw. Sci. Eng.*, vol. 13, pp. 1436–1457, 2026.
- [20] X. Chen, Z. Zhao, S. Mao, C. Wu, H. Zhang, and M. Bennis, "Age of semantics in cooperative communications: To expedite simulation towards real via offline reinforcement learning," *IEEE Trans. Netw. Sci. Eng.*, vol. 12, no. 4, pp. 3244–3258, 2025.
- [21] W. Pan, Z. Deng, X. Wang, P. Zhou, and W. Wu, "Optimizing the age of information for multi-source information update in internet of things," *IEEE Trans. Netw. Sci. Eng.*, vol. 9, no. 2, pp. 904–917, 2022.
- [22] A. Zakeri, M. Moltafet, and M. Codreanu, "Semantic-aware sampling and transmission in real-time tracking systems: A pomdp approach," *IEEE Trans. Commun.*, vol. 73, no. 7, pp. 4898–4913, 2025.
- [23] Y. Sun, E. Uysal-Biyikoglu, R. D. Yates, C. E. Koksall, and N. B. Shroff, "Update or wait: How to keep your data fresh," *IEEE Trans. Inf. Theory*, vol. 63, no. 11, pp. 7492–7508, 2017.
- [24] H. Hu, K. Xiong, Y. Lu, B. Gao, P. Fan, and K. B. Letaief, " α - β AoI penalty in wireless-powered status update networks," *IEEE Internet Things J.*, vol. 9, no. 1, pp. 474–484, 2022.
- [25] X. Cao, J. Wang, Y. Cheng, and J. Jin, "Optimal sleep scheduling for energy-efficient AoI optimization in industrial internet of things," *IEEE Internet Things J.*, vol. 10, no. 11, pp. 9662–9674, 2023.
- [26] T. Chang, X. Cao, and W. X. Zheng, "A lightweight sensor scheduler based on AoI function for remote state estimation over lossy wireless channels," *IEEE Trans. Automat. Contr.*, vol. 69, no. 3, pp. 1697–1704, 2024.
- [27] Y.-P. Hsu, E. Modiano, and L. Duan, "Scheduling algorithms for minimizing age of information in wireless broadcast networks with random arrivals," *IEEE Trans. Mobile Comput.*, vol. 19, no. 12, pp. 2903–2915, 2020.
- [28] H. Tang, J. Wang, Z. Tang, and J. Song, "Scheduling to minimize age of synchronization in wireless broadcast networks with random updates," *IEEE Trans. Wireless Commun.*, vol. 19, no. 6, pp. 4023–4037, 2020.
- [29] J. Liu, R. Zhang, A. Gong, and H. Chen, "Optimizing age of information in wireless uplink networks with partial observations," *IEEE Trans. Commun.*, vol. 71, no. 7, pp. 4105–4118, 2023.
- [30] J. Wang, X. Ren, S. Dey, and L. Shi, "Remote state estimation with usage-dependent Markovian packet losses," *Automatica*, vol. 123, p. 109342, 2021.
- [31] J. Wei and D. Ye, "Double threshold structure of sensor scheduling policy over a finite-state Markov channel," *IEEE Trans. Cybern.*, vol. 53, no. 11, pp. 7323–7332, 2023.
- [32] B. Yin, S. Zhang, and Y. Cheng, "Application-oriented scheduling for optimizing the age of correlated information: A deep-reinforcement-learning-based approach," *IEEE Internet Things J.*, vol. 7, no. 9, pp. 8748–8759, 2020.
- [33] J. Luo and N. Pappas, "Semantic-aware remote estimation of multiple Markov sources under constraints," *IEEE Trans. Commun.*, vol. 73, no. 11, pp. 11 093–11 105, 2025.
- [34] H. Wang, Y. Wang, X. Xie, and M. Li, "A scheduling scheme for minimizing age under delay tolerance in IoT systems with heterogeneous traffic," *IEEE Internet Things J.*, vol. 11, no. 9, pp. 16 902–16 914, 2024.
- [35] O. Ayan, S. Hirche, A. Ephremides, and W. Kellerer, "Optimal finite horizon scheduling of wireless networked control systems," *IEEE/ACM Trans. Networking*, vol. 32, no. 2, pp. 927–942, 2023.
- [36] X. Guo and Q. Zhu, "Average optimality for Markov decision processes in Borel spaces: A new condition and approach," *J. Appl. Probab.*, vol. 43, no. 2, pp. 318–334, 2006.
- [37] D. P. Bertsekas, *Dynamic Programming and Optimal Control*. Belmont, MA: Athena Scientific, 2007.
- [38] Y. Cui, V. K. N. Lau, and Y. Wu, "Delay-aware BS discontinuous transmission control and user scheduling for energy harvesting downlink coordinated MIMO systems," *IEEE Trans. Signal Process.*, vol. 60, no. 7, pp. 3786–3795, 2012.
- [39] S. Wu, K. Ding, P. Cheng, and L. Shi, "Optimal scheduling of multiple sensors over lossy and bandwidth limited channels," *IEEE Trans. Control Netw. Syst.*, vol. 7, no. 3, pp. 1188–1200, 2020.
- [40] D. Han, J. Wu, H. Zhang, and L. Shi, "Optimal sensor scheduling for multiple linear dynamical systems," *Automatica*, vol. 75, pp. 260–270, 2017.
- [41] C. Wu, Q. Chai, Y. Chen, L. Yin, and H. Zhu, "Remote state estimator design under the Round-Robin protocol," *Intl J Robust & Nonlinear*, vol. 34, no. 3, pp. 1828–1844, 2024.
- [42] A. S. Leong, D. E. Quevedo, D. Dolz, and S. Dey, "Transmission scheduling for remote state estimation over packet dropping links in the presence of an eavesdropper," *IEEE Trans. Automat. Contr.*, vol. 64, no. 9, pp. 3732–3739, 2019.
- [43] R. Cavazos-Cadena and L. I. Sennott, "Comparing recent assumptions for the existence of average optimal stationary policies," *Oper. res. lett.*, vol. 11, no. 1, pp. 33–37, 1992.
- [44] Z. Ren, P. Cheng, J. Chen, L. Shi, and H. Zhang, "Dynamic sensor transmission power scheduling for remote state estimation," *Automatica*, vol. 50, no. 4, pp. 1235–1242, 2014.